

Approximate Bayesian Computation with Statistical Distances for Model Selection

Clara Grazian^{1,2}

¹*Carlslaw Building, University of Sydney, Camperdown Campus, Sydney, Australia e-mail: clara.grazian@sydney.edu.au*

²*ARC Training Centre in Data Analytics for Resources and Environments (DARE), Sydney, Australia*

Abstract: Model selection is a key task in statistics, playing a critical role across various scientific disciplines. While no model can fully capture the complexities of a real-world data-generating process, identifying the model that best approximates it can provide valuable insights. Bayesian statistics offers a flexible framework for model selection by updating prior beliefs as new data becomes available, allowing for ongoing refinement of candidate models. This is typically achieved by calculating posterior probabilities, which quantify the support for each model given the observed data. However, in cases where likelihood functions are intractable, exact computation of these posterior probabilities becomes infeasible. Approximate Bayesian computation (ABC) has emerged as a likelihood-free method and it is traditionally used with summary statistics to reduce data dimensionality, however this often results in information loss difficult to quantify, particularly in model selection contexts. Recent advancements propose the use of full data approaches based on statistical distances, offering a promising alternative that bypasses the need for handcrafted summary statistics and can yield posterior approximations that more closely reflect the true posterior under suitable conditions. Despite these developments, full data ABC approaches have not yet been widely applied to model selection problems. This paper seeks to address this gap by investigating the performance of ABC with statistical distances in model selection. Through simulation studies and an application to toad movement models, this work explores whether full data approaches can overcome the limitations of summary statistic-based ABC for model choice.

MSC2020 subject classifications: Primary 62F15, 62-08; secondary 62C10.

Keywords and phrases: approximate Bayesian computation, model choice, animal behavior, full data approaches.

1. Introduction

The selection of a model that best explains a dataset or process is central to statistics and relevant across disciplines. While no model can fully capture all nuances in complex phenomena, approximating the true data-generating process (DGP) can yield valuable insights (Molnar et al., 2022). Importantly, the best model is not fixed; as new evidence arises, previously accepted models may require refinement or replacement (Gelman and Shalizi, 2013).

Bayesian statistics provides a natural framework for model selection. Bayes' theorem enables the updating of prior beliefs about candidate models as new data becomes available. Each model's support is quantified through its posterior probability, i.e. the probability of the model given the data, enabling probabilistic model comparison. The model with the highest posterior probability can be selected, or model averaging can be used to weigh models based on these probabilities (Raftery, 1995; Wasserman, 2000).

However, many models involve complex interdependencies or latent variables that render their likelihood functions intractable (Martin et al., 2024). In such cases, exact posterior probabilities cannot be computed, motivating likelihood-free methods such as approximate Bayesian computation (ABC). While ABC is typically used for parameter inference, it can also support model selection, provided all models can be simulated from. ABC estimates model support by weighting how often each model generates data that is "close enough" to the observed data, thus approximating its posterior probability.

To mitigate the curse of dimensionality, ABC often relies on low-dimensional summary statistics rather than comparing full datasets directly. However, this summarization can introduce information loss, particularly problematic for model selection where subtle differences between models may be important (Robert et al., 2011).

Other likelihood-free methods, such as Bayesian synthetic likelihood, variational Bayes, and integrated nested Laplace approximation, have also been developed to handle intractable models (Martin et al., 2024). These methods make different assumptions and approximations, and their suitability depends on the context and computational constraints. Compared to these approaches, ABC is especially flexible due to its minimal assumptions, but this flexibility comes at the cost of sensitivity to the choice of summaries.

To address the limitations of summary-based ABC, recent developments have introduced new versions of ABC methods: for example, Forbes et al. (2022) introduced a framework that constructs surrogate posteriors using finite Gaussian mixtures, employing inverse regression techniques and then utilizes distributional metrics to compare surrogate posteriors, while other ABC methods compare entire empirical distributions using statistical distances (Park et al., 2016; Bernton et al., 2019; Nguyen et al., 2020; Frazier, 2020). These methods, sometimes called "full data approaches" (Drovandi and Frazier, 2022), eliminate the need to define summary statistics and aim to approximate the exact posterior. However, their use for model selection remains underexplored, particularly in cases where competing models are similar.

Another direction to improve ABC has involved machine learning, especially deep learning, to learn informative low-dimensional summaries automatically. Approaches such neural network adjustments (Blum and François, 2010), and summary learning via deep networks (Sheehan and Song, 2016; Jiang et al., 2017) have shown promise in parameter inference. Yet these methods typically require large simulated datasets and can suffer when the training model is misspecified. In contrast, ABC directly compares simulated datasets to the observed one, providing a form of robustness to model misspecification. Theoretical work

by Frazier et al. (2020), for instance, has shown how ABC posteriors behave under such conditions, offering insights into its relative stability where deep learning approaches may fail.

While deep learning has been applied to related problems such as kinetic model classification (Burés and Larrosa, 2023), such tasks differ from true model selection, especially in overlapping model spaces. ABC, by simulating under each model and comparing to observed data, offers a principled framework for likelihood-free model comparison. In this paper, we evaluate the performance of full data ABC methods for model selection, comparing their effectiveness to summary-based ABC and deep learning classifiers. Our results demonstrate that full data ABC offers a flexible and robust approach to model choice when likelihoods are unavailable.

The remainder of the paper is structured as follows. Section 2 reviews Bayesian model selection and introduces ABC. Section 3 discusses the use of ABC for model choice, highlighting its challenges and introducing full data methods, with a theoretical justification focused on the Wasserstein distance. Section 4 presents a simulation study comparing full data, summary-statistics-based ABC approaches, and deep learning alternatives. Section 5 applies these methods to the toad movement models of Marchand et al. (2017). Finally, Section 6 concludes the paper. The code to replicate the simulations of Section 4 is available at <https://github.com/bayesgra/ABC-MC>.

2. Background

2.1. Notation and Setting

Let $\mathbf{y} = (y_1, \dots, y_n)^T \in \mathcal{Y}^n \subseteq \mathbb{R}^n$ denote the observed data, assumed to be generated from an unknown true distribution $P_{\theta_0}^{(n)}$ within a model family $\mathcal{P} = \{P_{\theta}^{(n)} : \theta \in \Theta \subseteq \mathbb{R}^d\}$. The assumed model M in this family is parameterized by θ with prior distribution $\pi(\theta)$, yielding a likelihood function $p(\mathbf{y}|\theta)$ and posterior distribution $\pi(\theta|\mathbf{y})$ via Bayes' theorem. The marginal likelihood or model evidence is defined as $p(\mathbf{y}) = \int_{\Theta} p(\mathbf{y}|\theta)\pi(\theta)d\theta$.

When the prior beliefs instead concerns a set of K candidate models M_1, \dots, M_K , each model M_k has parameters $\theta_k \in \Theta_k \subseteq \mathbb{R}^{d_k}$ with prior distribution $\pi_k(\theta_k)$ and likelihood function $p_k(\mathbf{y}|\theta_k) = p(\mathbf{y}|\theta_k, M_k)$. Models are assigned prior probabilities $\pi(M_k) = \pi(M = M_k)$ such that $\sum_{k=1}^K \pi(M_k) = 1$. The posterior probability for model M_k is:

$$\pi(M_k|\mathbf{y}) = \frac{p_k(\mathbf{y})\pi(M_k)}{\sum_{j=1}^K p_j(\mathbf{y})\pi(M_j)} \quad \forall k = 1, \dots, K,$$

where $p_k(\mathbf{y})$ is the marginal likelihood under model M_k . The true DGP $P_{M_0, \theta_0}^{(n)}$ is assumed to belong to the broader set $\mathcal{P} = \{P_{M_k, \theta_k}^{(n)} \mid \theta_k \in \Theta_k \subseteq \mathbb{R}^{d_k}, k \in \{1, \dots, K\}\}$.

To compare two models M_i and M_j , the Bayes Factor

$$B_{ij}(\mathbf{y}) = \frac{p_i(\mathbf{y})}{p_j(\mathbf{y})} = \frac{\pi(M_i|\mathbf{y})}{\pi(M_j|\mathbf{y})} \bigg/ \frac{\pi(M_i)}{\pi(M_j)}.$$

quantifies the change in relative belief in favor of M_i over M_j due to the observed data.

2.2. Approximate Bayesian Computation

Obtaining posterior distributions for model selection can be analytically intractable. When likelihood functions are available, Markov chain Monte Carlo (MCMC) methods enable posterior estimation and model comparison via Bayes factors, but these methods can be computationally intensive and require careful tuning (Han and Carlin, 2001). This has motivated the development of alternative, less formal methods for Bayesian model comparison that are more feasible in complex settings (Morey et al., 2011). In many complex systems, such as finance (Peters et al., 2015), hydrology (Smith et al., 2014), and ecology (Marchand et al., 2017), the likelihood is unavailable or expensive to compute, and standard Monte Carlo or MCMC methods struggle with scalability in large or high-dimensional data (Bardenet et al., 2017).

ABC addresses this challenge by approximating the posterior distribution when the likelihood $p(\mathbf{y}|\boldsymbol{\theta})$ is intractable. The basic rejection ABC (Pritchard et al., 2000) involves simulating a dataset $\mathbf{z} = (z_1, \dots, z_n)^T$ from a parameter $\boldsymbol{\theta}^*$ drawn, for example, from the prior distribution, comparing summaries $\boldsymbol{\eta}(\mathbf{z})$ and $\boldsymbol{\eta}(\mathbf{y})$ via a distance $\rho(\cdot, \cdot)$, and accepting $\boldsymbol{\theta}^*$ if the distance is below a tolerance ε . A step-by-step algorithm can be found in Appendix A. This method targets an approximate posterior distribution $\pi_\varepsilon(\boldsymbol{\theta}|\boldsymbol{\eta}(\mathbf{y}))$, which depends on summary statistics that are typically not sufficient. Several computationally efficient ABC extensions have been proposed (Beaumont et al., 2002; Marjoram et al., 2003; Sisson et al., 2007; Beaumont et al., 2009; Del Moral et al., 2011).

The choice of low-dimensional, informative summary statistics is critical. Barber et al. (2015) show the mean squared error (MSE) of ABC scales as $\mathcal{O}(N^{-4/(q+4)})$, where q is the dimension of the summary statistic. Strategies for summary selection include subset selection (Joyce and Marjoram, 2008; Nunes and Balding, 2010), projection methods (Fearnhead and Prangle, 2012), and auxiliary models such as Gaussian mixtures (Wilson et al., 2008; Drovandi et al., 2011; Gleim and Pigorsch, 2013; Drovandi et al., 2015; Martin et al., 2019).

To circumvent summary selection, full data ABC methods compare empirical distributions of the observed and simulated data directly using statistical distances. In this approach (Drovandi and Frazier, 2022), the distance metric $\rho(\cdot, \cdot)$ is replaced with a discrepancy measure $\mathcal{D}(\cdot, \cdot)$ applied to empirical measures $\mu_{\boldsymbol{\theta}_0}$ and $\mu_{\boldsymbol{\theta}^*}$, constructed from observed and simulated samples. Here, $\mu_{\boldsymbol{\theta}_0}$ denotes the measure associated with the true distribution $P_{\boldsymbol{\theta}_0}^{(n)}$ and $\mu_{\boldsymbol{\theta}^*}$ is used to indicate the measure associated with the simulated data's distribution $P_{\boldsymbol{\theta}^*}^{(n)} \in \mathcal{P}$,

respectively. As $P_{\theta_0}^{(n)}$ is unavailable, the empirical distributions of \mathbf{y} and \mathbf{z} replace the true measures, defined as $\hat{\mu}_{\theta_0} = n^{-1} \sum_{i=1}^n \delta_{y_i}$ and $\hat{\mu}_{\theta^*} = n^{-1} \sum_{i=1}^n \delta_{z_i}$ respectively, where δ_x is the Dirac measure on $x \in \mathcal{Y}$. A corresponding rejection algorithm using statistical distances is also detailed in Appendix A.

Legramanti et al. (2025) provide theoretical justification for these methods using integral probability semimetrics (IPS), such as the Wasserstein distance or maximum mean discrepancy (MMD), and Rademacher complexity, showing uniform concentration bounds on the ABC posterior distribution even under model misspecification and non-i.i.d. (independent and identically distributed) data. Empirical work by Drovandi and Frazier (2022) shows that full data ABC can match or outperform summary-based ABC in parameter inference, with certain discrepancies better suited to specific problems. However, model selection using discrepancy-based ABC remains underexplored and is the focus of this work.

3. Approximate Bayesian Computation for Model Selection

In Bayesian model selection, ABC estimates the posterior model probability $\pi(M_k|\mathbf{y})$ using the acceptance rate under model M_k , assuming data $\mathbf{z} \sim P_{M_k, \theta_k}^{(n)}$ with likelihood $p_k(\mathbf{z}|\theta_k)$. The ABC model choice (ABC-MC) approach, formally introduced by Grelaud et al. (2009) to compare Gibbs random fields models with different dependence structures and presented in Algorithm 3 in Appendix A, has since been applied in a range of fields including population genetics (Estoup et al., 2004; Miller et al., 2005), archaeology (Crema et al., 2014), and evolutionary biology (Bennett et al., 2016; Prangle et al., 2014), and presented using sequential Monte Carlo in Didelot et al. (2011).

However, model choice via ABC introduces challenges beyond standard inference. Robert et al. (2011) showed that even with sufficient statistics and vanishing tolerance $\varepsilon \rightarrow 0$, the ABC Bayes factor between two models $B_{ij}^\eta(\mathbf{y})$, may fail to converge to the true Bayes factor $B_{ij}(\mathbf{y})$, due to the unbounded correction ratio

$$\frac{B_{ij}(\mathbf{y})}{B_{ij}^\eta(\mathbf{y})} = \frac{g_i(\mathbf{y})}{g_j(\mathbf{y})},$$

where $g_\ell(\mathbf{y}) = p_\ell(\mathbf{y}|\theta_\ell)/p_\ell^\eta(\boldsymbol{\eta}(\mathbf{y})|\theta_\ell)$, with $p_\ell^\eta(\boldsymbol{\eta}(\mathbf{y})|\theta_\ell)$ the likelihood function for the summary statistic under model $\ell = i, j$, reflects the discrepancy between full and summary likelihoods. A notable exception is described in Grelaud et al. (2009), where sufficiency is preserved across models.

Marin et al. (2013) derived sufficient conditions for summary statistics to ensure consistency in ABC model selection, but these require that only one model aligns with the observed summaries, which may be unrealistic. Alternatives for constructing approximately sufficient summaries include a two-stage selection method (Barnes et al., 2012) and projection-based approaches (Prangle et al., 2014).

3.1. ABC-MC with Statistical Distances

To incorporate statistical distances into model selection, the ABC distance metric $\rho(\cdot, \cdot)$ is replaced with a discrepancy measure $\mathcal{D}(\cdot, \cdot)$ that operates on the probability measures of the observed data \mathbf{y} and simulated data \mathbf{z} . We denote μ_{0, θ_0} as the measure associated with the true distribution $P_{M_0, \theta_0}^{(n)}$, and $\mu_{k^*, \theta_{k^*}}$ as the measure associated with the simulated data's distribution $P_{M_{k^*}, \theta_{k^*}}^{(n)} \in \mathcal{P}$. The empirical distributions of \mathbf{y} and \mathbf{z} replace the true measures, and are similarly defined as $\hat{\mu}_{0, \theta_0} = n^{-1} \sum_{i=1}^n \delta_{y_i}$ and $\hat{\mu}_{k^*, \theta_{k^*}} = n^{-1} \sum_{i=1}^n \delta_{z_i}$ respectively. This forms the basis of Algorithm 1.

Algorithm 1 Discrepancy-based ABC-MC

- 1: **Input:** Given a set of observations $\mathbf{y} = (y_1, \dots, y_n)^T$, a set of possible models $\{M_1, M_2, \dots, M_K\}$, a tolerance level ε , and a discrepancy metric $\mathcal{D}(\cdot, \cdot)$:
 - 2: **for** $i = 1, \dots, N$ **do**
 - 3: **repeat**
 - 4: Generate M_{k^*} from $\pi(M_k)$, $k = 1, \dots, K$.
 - 5: Generate θ_{k^*} from $\pi_{k^*}(\theta_{k^*})$.
 - 6: Generate $\mathbf{z} = (z_1, \dots, z_n)^T$ from $P_{M_{k^*}, \theta_{k^*}}^{(n)}$.
 - 7: **until** $\mathcal{D}(\hat{\mu}_{0, \theta_0}, \hat{\mu}_{k^*, \theta_{k^*}}) \leq \varepsilon$,
 - 8: Set $M^{(i)} = M_{k^*}$ and $\theta^{(i)} = \theta_{k^*}$.
 - 9: **end for**
 - 10: **Output:** A set of values $(M^{(1)}, \dots, M^{(N)})$ and $(\theta^{(1)}, \dots, \theta^{(N)})$ from $\pi_\varepsilon(M_k | \mathbf{y})$ and $\pi_{\varepsilon, k}(\theta_k | \mathbf{y}, M_k)$, for $k = 1, \dots, K$, respectively.
-

This is the first study to propose Algorithm 1 and to systematically explore its use with various discrepancy measures. We now provide a list of statistical distance metrics that are suitable for use with this approach. They all fall under the IPS class, so the results of Legramanti et al. (2025) apply for parameter inference. These metrics will be employed in both an extensive simulation study and a real data application, presented in Sections 4 and 5, to assess the effectiveness of full data ABC approaches for model selection tasks.

The maximum mean discrepancy (MMD) (Park et al., 2016) compares embedded empirical distributions in a reproducing kernel Hilbert space, using a kernel $g : \mathcal{Y} \times \mathcal{Y} \rightarrow \mathbb{R}$,

$$MMD^2(\mu_{0, \theta_0}, \mu_{k^*, \theta_{k^*}}) = \mathbb{E}[g(y_1, y_2)] + \mathbb{E}[g(z_1, z_2)] - 2\mathbb{E}[g(y_1, z_1)].$$

The unbiased empirical estimate is:

$$\begin{aligned} MMD^2(\hat{\mu}_{0, \theta_0}, \hat{\mu}_{k^*, \theta_{k^*}}) &= \frac{1}{n(n-1)} \sum_{i=1}^n \sum_{j \neq i}^n g(y_i, y_j) + \frac{1}{n(n-1)} \sum_{i=1}^n \sum_{j \neq i}^n g(z_i, z_j) + \\ &\quad - \frac{2}{n^2} \sum_{i=1}^n \sum_{j=1}^n g(y_i, z_j). \end{aligned} \tag{1}$$

A common choice of kernel is the Gaussian kernel, $g(y, z) = \exp\left(-\frac{\|y-z\|_2^2}{2\sigma}\right)$, which produces an MMD that attempts to match all moments between the two distributions. A similar approach using the energy distance, a specific case of MMD where the Euclidean distance is used as the kernel function, was explored by [Nguyen et al. \(2020\)](#).

[Bernton et al. \(2019\)](#) proposed using the Wasserstein distance in ABC. For univariate data and assuming that $P_{M_0, \theta_0}^{(n)}$ and $P_{M_{k^*}, \theta_{k^*}}^{(n)}$ have finite p -th moment with $p \geq 1$, the p -Wasserstein distance between these measures is given by

$$\mathcal{W}_p(\mu_{0, \theta_0}, \mu_{k^*, \theta_{k^*}}) = \left(\int_0^1 |F_{\mu_{0, \theta_0}}^{-1}(\lambda) - F_{\mu_{k^*, \theta_{k^*}}}^{-1}(\lambda)|^p d\lambda \right)^{1/p},$$

where $F_{\mu_{0, \theta_0}}(\cdot)$ and $F_{\mu_{k^*, \theta_{k^*}}}(\cdot)$ are the cumulative distribution functions of $P_{M_0, \theta_0}^{(n)}$ and $P_{M_{k^*}, \theta_{k^*}}^{(n)}$, respectively. The empirical p -Wasserstein distance, with $p = 1$, is computed by comparing order statistics:

$$\mathcal{W}_1(\hat{\mu}_{0, \theta_0}, \hat{\mu}_{k^*, \theta_{k^*}}) = n^{-1} \sum_{i=1}^n |y_{(i)} - z_{(i)}|. \quad (2)$$

Although theoretically appealing because it can lead to an ABC algorithm that approximates the true posterior distribution arbitrarily well as $\varepsilon \rightarrow 0$, its performance may degrade when data quantiles are insensitive to parameters changes ([Drovandi and Frazier, 2022](#)).

The Cramér–von Mises (CvM) distance ([Frazier, 2020](#)), motivated by minimum distance estimation ([Donoho and Liu, 1988](#)), which provides nice properties such as yielding robust and potentially efficient point estimators, measures the L_2 difference between the empirical CDF $\hat{F}_{\mu_{k^*}, \theta_{k^*}}$ and the CDF of the theoretical distribution $F_{\mu_{0, \theta_0}}$

$$\mathcal{C}^2(\mu_{0, \theta_0}, \mu_{k^*, \theta_{k^*}}) = \int_{\mathcal{Y}} \left[\hat{F}_{\mu_{k^*}, \theta_{k^*}}(y) - F_{\mu_{0, \theta_0}}(y) \right]^2 dF_{\mu_{0, \theta_0}}(y).$$

It is estimated by:

$$\mathcal{C}^2(\hat{\mu}_{0, \theta_0}, \hat{\mu}_{k^*, \theta_{k^*}}) = \frac{U}{2n^2} - \frac{4n^2 - 1}{12n}, \quad (3)$$

where U involves the ranks of \mathbf{y} and \mathbf{z} in their pooled sample.

3.2. Theoretical justification

Consider the version of Algorithm 1 using the Wasserstein distance and a sequence $\varepsilon_n \rightarrow 0$ of threshold varying with the sample size n , and define this algorithm ABC-Wass. Then, the ABC posterior probability of model $M_{k^*} \in \{M_1, \dots, M_K\} = \mathcal{M}$ is

$$\pi_{\varepsilon_n}(M_{k^*} | \mathbf{y}) \propto \pi(M_{k^*}) \int_{\Theta_{k^*}} \pi(\theta_{k^*} | M_{k^*}) \mathbb{P} \{ \mathcal{W}_p(\hat{\mu}_{0, \theta_0}, \hat{\mu}_{k^*, \theta_{k^*}}) \leq \varepsilon_n \} d\theta_{k^*}. \quad (4)$$

where the the left hand side is normalized over models.

The expression $\mathbb{P}(\cdot)$ refers to the random probability over simulations that a sample $\boldsymbol{\theta}_{k^*}$ under model M_{k^*} yields a Wasserstein distance smaller or equal to a threshold ε_n . This is the noisy version of ABC considered in the framework of [Bernton et al. \(2019\)](#).

Under regularity conditions, ABC-Wass yields consistent parameter estimation ([Bernton et al., 2019](#)). This property extends to model selection via [Theorem 3.1](#), when the candidate models are well-separated in the Wasserstein sense, i.e. they generate distinguishable empirical distributions, and the Wasserstein distance between empirical samples is accurate enough. To guarantee this, the acceptance threshold must be taken as a sequence $\varepsilon_n \rightarrow 0$ as $n \rightarrow \infty$, since with growing sample size the empirical distributions concentrate around their population laws, and a fixed tolerance ε would allow incorrect models to pass the ABC criterion whenever their Wasserstein distance from the true model is below ε .

Moreover, we restrict attention to the case of i.i.d. observations. This choice aligns with [Assumption \(A4\)](#) of [Theorem 3.1](#) on the convergence of Wasserstein distances, which holds under mild conditions, e.g. existence of finite p -th moments, in the i.i.d. setting. Recently, [Legramanti et al. \(2025\)](#) extended certain convergence results to non-i.i.d. contexts, including time series models, but we leave such extensions for future work.

Theorem 3.1 (Model Selection Consistency of ABC-Wass). *Assume:*

(A1) (*Identifiability*): For all $M_{k^*} \neq M_0$, there exists $\delta_{k^*} > 0$ such that

$$\inf_{\boldsymbol{\theta}_{k^*} \in \Theta_{k^*}} \mathcal{W}_p(P_{M_0, \boldsymbol{\theta}_0}^{(n)}, P_{M_{k^*}, \boldsymbol{\theta}_{k^*}}^{(n)}) > \delta_{k^*}.$$

(A2) (*Prior Positivity*): $\pi(M_0) > 0$ and $\pi_{M_0}(\boldsymbol{\theta}_0) > 0$.

(A3) (*Tail Behavior*): For each $M_{k^*} \neq M_0$, let $\mathcal{B}_{\delta_{k^*}} = \{\boldsymbol{\theta}_{k^*} \in \Theta_{k^*} : \mathcal{W}_p(P_{M_0, \boldsymbol{\theta}_0}, P_{M_{k^*}, \boldsymbol{\theta}_{k^*}}) \leq 2\delta_{k^*}/3\}$, where δ_{k^*} is as in [Assumption \(A1\)](#). Then, for any sequence $\varepsilon_n \rightarrow 0$ with $\varepsilon_n < \delta_{k^*}/2$ for large n

$$\int_{\Theta_{k^*} \setminus \mathcal{B}_{\delta_{k^*}}} \pi_{M_{k^*}}(\boldsymbol{\theta}_{k^*}) \cdot \mathbb{P}(\mathcal{W}_p(\hat{\mu}_0, \boldsymbol{\theta}_0, \hat{\mu}_{k^*}, \boldsymbol{\theta}_{k^*}) \leq \varepsilon_n) d\boldsymbol{\theta}_{k^*} \rightarrow 0 \quad \text{as } n \rightarrow \infty.$$

(A4) (*Empirical Convergence*): $\mathcal{W}_p(\hat{\mu}_0, \boldsymbol{\theta}_0, P_{M_0, \boldsymbol{\theta}_0}^{(n)}) \rightarrow 0$ and $\mathcal{W}_p(\hat{\mu}_{k^*}, \boldsymbol{\theta}_{k^*}, P_{M_{k^*}, \boldsymbol{\theta}_{k^*}}^{(n)}) \rightarrow 0$ almost surely as $n \rightarrow \infty$, and $\Delta_n := \sup_{M_{k^*}, \boldsymbol{\theta}_{k^*}} \mathbb{E}[\mathcal{W}_p(\hat{\mu}_{k^*}, \boldsymbol{\theta}_{k^*}, P_{M_{k^*}, \boldsymbol{\theta}_{k^*}}^{(n)})]$ satisfies $\Delta_n = o(\varepsilon_n)$.

Then, for any sequence $\varepsilon_n \rightarrow 0$ such that $\varepsilon_n < \min_{k^*} \delta_{k^*}/2$,

$$\pi_{\varepsilon_n}(M_0 \mid \mathbf{y}) \xrightarrow{P} 1 \quad \text{as } n \rightarrow \infty.$$

The proof of [Theorem 3.1](#) is provided in [Appendix B](#) of the [Supplementary Material](#). [Theorem 3.1](#) states that, under suitable conditions, the ABC posterior over models assigns probability one to the true model M_0 as the sample size

increases. Assumption (A1) ensures that for any incorrect model $M_{k^*} \neq M_0$ and any parameter $\theta_{k^*} \in \Theta_{k^*}$, the Wasserstein distance between the simulated data distribution $P_{M_{k^*}, \theta_{k^*}}^{(n)}$ and the true distribution $P_{M_0, \theta_0}^{(n)}$ is bounded below by some fixed $\delta_{k^*} > 0$. This guarantees that no parameter in a wrong model can generate data arbitrarily close to the true data; without this, a wrong model might mimic the observed data. Assumption (A2) requires that both the model prior and the parameter prior assign positive mass to neighborhoods of the true model and true parameter. Assumption (A3) ensures that parameter values far (in Wasserstein distance) to $P_{M_0, \theta_0}^{(n)}$ cannot produce empirical measures within the small threshold with non-negligible prior mass. In other words, the prior must decay sufficiently fast in regions where the Wasserstein distance between the simulated and true distribution is large. Finally, Assumption (A4) holds for i.i.d. observations and in cases with a finite p -th moment.

Theorem 3.2 (Robustness to Model Misspecification). *Let the true data distribution $P_{M_0, \theta_0}^{(n)}$ be misspecified with respect to the candidate set*

$$\{P_{M_k, \theta_k}^{(n)} : M_k \in \mathcal{M}, \theta_k \in \Theta_k\}.$$

Suppose Assumptions (A1)-(A4) hold, and let the ABC tolerance decreases to zero, i.e. $\varepsilon_n \rightarrow 0$, at a rate slower than the stochastic convergence of the Wasserstein distance $\mathcal{W}_p(\hat{\mu}_0, P_{M_0, \theta_0}^{(n)})$. Then the ABC-Wass posterior asymptotically concentrates on the model-parameter pair

$$(M^\dagger, \theta^\dagger) = \arg \min_{M_k \in \mathcal{M}, \theta_k \in \Theta_k} \mathcal{W}_p(P_{M_0, \theta_0}^{(n)}, P_{M_k, \theta_k}^{(n)}).$$

The proof of Theorem 3.2 is available in Appendix C of the Supplementary Material. This result shows that, under model misspecification, ABC-Wass asymptotically selects the model whose distribution is closest to the true data distribution in the Wasserstein metric.

We evaluate full data ABC approaches under the i.i.d. assumption in Sections 4.2–4.3 and extend the analysis to dependent data in Sections 4.4–5. Although Wasserstein, MMD, and CvM distances are traditionally defined for i.i.d. samples, they can be adapted to dependence, for example via time-aware kernels or block structures. Legramanti et al. (2025) established that, under suitable regularity conditions, the ABC posterior based on such distances retains uniform convergence properties in the temporally dependent setting.

4. Simulation Study

The goal of this section is to assess ABC’s empirical performance with various distances and to compare it with other methods.

This section applies ABC with statistical distances (Algorithm 1), specifically MMD (1), Wasserstein (2), and CvM (3), to several simulated model selection problems, comparing performance against summary-based ABC (Algorithm 3,

Appendix A), in which problem-specific summary statistics are used. The full data approaches are referred to as ABC-MMD, ABC-Wass, and ABC-CvM, while ABC-Stat denotes the summary-based method.

Each experiment is repeated 100 times for sample sizes $n = 100$ and $n = 1000$ in Section 4.1, 4.2 and 4.3, and it is repeated 100 times for a sample sizes replicating the true data example of Section 5 in Section 4.4. For each observed dataset, 10^6 simulations are generated to approximate posterior model probabilities and model-specific parameter posteriors for all examples, except the one described in Section 4.4. Model priors are taken as uniform, $\pi(M = M_k) = 1/K$ for $k = 1, \dots, K$, and parameter priors are defined individually for each example. The distance threshold ε is not fixed a priori; instead, following Biau et al. (2015), it is chosen as the q -th percentile of the simulated distances, retaining only the closest $q\%$ of simulations. The chosen q values are reported for each example.

Across all examples, performance is assessed using: (i) the estimated probability of selecting the correct model; (ii) the average posterior means of the parameters and their mean squared errors (MSEs); (iii) classification accuracy summarised through confusion matrices (shown in the Appendixes); and (iv) boxplots of the posterior probability of selecting the correct model across repetitions (shown in the Appendixes).

To further assess ABC’s effectiveness in model choice and parameter inference, we compare it with a deep neural network (NN) trained on the same models and tested on the same 100 datasets. The network performs multi-task learning: classification (model selection) with categorical cross-entropy loss and regression (parameter estimation) using MSE loss. Loss weights are 1.0 (classification) and 0.5 (regression), prioritizing model identification. The architecture comprises five fully connected layers.

The neural network trains on 10^6 datasets (80% for training, 20% for testing) generated using the true parameters, assuming the true model is included in the simulation design. In contrast, ABC simulates from prior distributions and selects samples closest to the observed data using distance metrics, making it more flexible and less assumption-dependent, especially when the true model or parameters are unknown.

Finally, we include two additional methods for comparison: (1) the semi-automatic summary selection method (ABC-SA) of Prangle et al. (2014), implemented in the `abctools` R package (Nunes and Prangle, 2015); and (2) the classification-based ABC using quadratic discriminant analysis (ABC-QDA) from Gutmann et al. (2018), originally developed for parameter inference rather than model selection. We select QDA as the classification algorithm because Gutmann et al. (2018) demonstrated its robustness across multiple examples. To the best of our knowledge, this approach has not previously been proposed for model selection.

4.1. Normal Mean Hypothesis Test

We assess ABC using distance metrics for model choice in a simple normal-data setting. Let $\mathbf{y} = (y_1, \dots, y_n)^T$ be i.i.d. with $y_i \sim N(\theta, \sigma^2)$, assuming $\sigma^2 = 1$. The competing models correspond to $H_0 : \theta = \tilde{\theta}$ versus $H_1 : \theta \neq \tilde{\theta}$.

Synthetic datasets are generated from the true model $\mathcal{N}(\theta_0, 1)$ with $\theta_0 \in \{0.0, 0.1, 0.2, 0.3, 0.4, 0.5\}$, allowing evaluation of method performance as the true mean departs from $\tilde{\theta} = 0$. For each value of θ_0 , 100 datasets are simulated and analyzed using the seven methods described above for model selection and parameter inference. Under H_1 , the prior is $\theta \sim N(\tilde{\theta}, 100)$, providing a weakly informative prior; under H_0 , θ is fixed at $\tilde{\theta} = 0$.

For this simple normal example with known variance, the Bayes factor B_{01} can be computed analytically (Robert, 2007, Chapter 5). While we do not use it in our evaluation, this example provides a context where the ABC procedure can, in principle, be compared to exact Bayesian inference. For ABC-Stat, we use the sufficient statistic $\eta(\mathbf{y}) = \bar{y}$ and the Euclidean distance.

We first assess each method’s ability to correctly identify the data-generating model. Performance is summarized using the estimated probability of selecting H_0 across different values of θ_0 (Table 1), and confusion matrices and boxplots of posterior probabilities (Appendix D of the Supplementary Material). ABC methods based on distance metrics correctly identify H_0 in all cases, indicating good control of false positives. The transition is gradual: for small deviations from zero (e.g., $\theta_0 = 0.1$), the classifier shows limited power, but confidence in selecting H_1 grows as the true mean increases. When $\theta_0 \geq 0.4$, H_1 is selected most of the time, reaching around 95% selection accuracy at $\theta_0 = 0.5$. ABC-SA follows a similar pattern but tends to select H_0 more often than the full data ABC approaches when the true mean increases. ABC-QDA selects H_0 in nearly all cases, while NN shows approximately random model selection, with probabilities close to 50% for both hypotheses.

We further evaluate posterior inference quality for θ by computing the MSE between the posterior mean and the true value θ_0 across repetitions (Table 1). For each dataset, the posterior mean is computed from the model selected as most probable by each method. Results show that MSE is generally low, with the smallest values observed when $\theta_0 = 0$ and $\theta_0 = 0.5$, consistent with improved classification accuracy for these values. When the true mean is small but non-zero, posterior distributions for all methods retain substantial mass near zero, reflecting limited information in the data to distinguish between models. ABC-SA and ABC-QDA exhibit larger MSE than the distance-based ABC methods, while NN estimation is further affected by the difficulty in correctly identifying the model.

All methods perform similarly when the sample size is $n = 1,000$, showing minimal differences in both model selection and parameter estimation. ABC methods also yield comparable results across smaller tolerance thresholds; therefore, these additional results are omitted.

These results demonstrate that ABC with distance metrics provides reliable performance for both model selection and parameter estimation, comparable to

		ABC				NN	ABC	
		CvM	MMD	Wass	Stat		SA	QDA
$\theta_0 = 0.0$	$\Pr(\theta = 0)$	0.975	0.976	0.975	0.973	0.500	0.976	0.981
	$\hat{\theta}$	0.000	0.000	0.000	0.002	0.049	0.000	0.000
	MSE	0.000	0.000	0.000	0.001	0.002	0.000	0.000
$\theta_0 = 0.1$	$\Pr(\theta = 0)$	0.931	0.933	0.929	0.921	0.503	0.948	0.974
	$\hat{\theta}$	0.007	0.006	0.007	0.010	0.049	0.000	0.000
	MSE	0.011	0.011	0.011	0.011	0.002	0.010	0.010
$\theta_0 = 0.2$	$\Pr(\theta = 0)$	0.788	0.796	0.789	0.760	0.495	0.847	0.955
	$\hat{\theta}$	0.046	0.042	0.042	0.048	0.104	0.010	0.000
	MSE	0.037	0.037	0.038	0.038	0.009	0.037	0.040
$\theta_0 = 0.3$	$\Pr(\theta = 0)$	0.522	0.543	0.519	0.459	0.499	0.671	0.934
	$\hat{\theta}$	0.147	0.144	0.149	0.168	0.149	0.141	0.000
	MSE	0.062	0.061	0.060	0.056	0.023	0.096	0.090
$\theta_0 = 0.4$	$\Pr(\theta = 0)$	0.210	0.236	0.203	0.157	0.503	0.450	0.902
	$\hat{\theta}$	0.344	0.335	0.345	0.364	0.000	0.285	0.000
	MSE	0.039	0.041	0.038	0.034	0.160	0.125	0.160
$\theta_0 = 0.5$	$\Pr(\theta = 0)$	0.056	0.067	0.050	0.031	0.501	0.263	0.870
	$\hat{\theta}$	0.494	0.489	0.497	0.506	0.000	0.359	0.000
	MSE	0.022	0.025	0.020	0.016	0.250	0.125	0.250

TABLE 1

Summary of results for the normal model across repetitions. For each true mean, the table reports the average probability of selecting hypothesis H_0 , the average posterior mean, and the corresponding MSE over all repetitions. For all ABC methods, $q\% = 1\%$ is used. Similar results are obtained with lower percentiles.

ABC-Stat using sufficient summary statistics. The comparison with other ABC algorithms and with NN in this simple example highlights the limitations of those methods and illustrates the advantages of full data ABC approaches for model selection problems.

4.2. Exponential Family Model Selection

In this example, we adopt the same model setup as in Marin et al. (2016) and consider three models from the exponential family for which the marginal likelihoods are available in closed form, allowing for analytical computation of the Bayes factors and posterior model probabilities. In our study, these quantities are not used, but we retain the model specification to facilitate comparison with their results.

Model M_1 assumes the data follow an exponential distribution with rate parameter θ , $y_i \stackrel{\text{i.i.d.}}{\sim} \text{Exp}(\theta)$, $i = 1, \dots, n$, with prior $\theta \sim \text{Exp}(1)$. Model M_2 specifies a log-normal distribution with location parameter θ and dispersion fixed at 1, $y_i \stackrel{\text{i.i.d.}}{\sim} \mathcal{LN}(\theta, 1)$, with prior $\theta \sim N(0, 1)$. Model M_3 assumes a gamma distribution with shape fixed at 2 and unknown rate parameter θ , $y_i \stackrel{\text{i.i.d.}}{\sim} \text{Ga}(2, \theta)$, with prior $\theta \sim \text{Exp}(1)$.

With these distributions belonging to the exponential family, the following

choice of summary statistics for ABC-Stat is sufficient for each model and across models in the sense of [Marin et al. \(2013\)](#). This means that, for the model choice problem, no information is lost by replacing the full dataset with these summaries:

$$\boldsymbol{\eta}(\mathbf{y}) = \left(\sum_{i=1}^n y_i, \sum_{i=1}^n \log y_i, \sum_{i=1}^n \log^2 y_i \right).$$

To assess the consistency of each ABC method, we fix θ when generating the observed data so that the true expected value under each model equals 2. This corresponds to $\theta = 1/2$ for M_1 , $\theta = \log 2 - 1/2$ for M_2 , and $\theta = 1$ for M_3 . [Figure 1](#) compares the densities of these models, showing that they are quite similar. Such similarity makes model selection more challenging, requiring low distance thresholds to achieve accurate results. Therefore, we present directly results using the 0.1% distance-quantile threshold.

Given the positive skewness observed in the densities, we apply log-transformations to both observed and simulated data for ABC-MMD and ABC-Wass. This follows the approach in [Drovandi and Frazier \(2022\)](#) for parameter estimation in skewed datasets. Since the CvM distance is invariant to monotonic transformations, no transformation is applied for ABC-CvM.

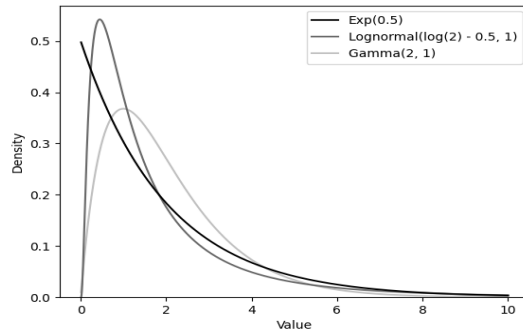


Figure 1: Comparison of the true data distributions for each model, with parameters set to $\theta = 1/2$ for M_1 , $\theta = \log 2 - 1/2$ for M_2 , and $\theta = 1$ for M_3 . These values give each model a mean of 2.

Results are summarised in [Table 2](#) and [Appendix E](#) of the Supplementary Material. When the true model is M_1 or M_2 , achieving high posterior probability for the correct model is challenging in some cases, whereas M_3 is generally identified with higher confidence by all methods. Applying a log transformation to the data improves the performance of ABC-Wass and ABC-MMD, enabling them to match the accuracy of ABC-Stat (with a posterior probability of the correct model close to one). ABC-Stat consistently achieves near-exact results. Without log transformations, MMD and Wasserstein performed similarly to CvM, with noticeably higher classification error. This is a significant observation, showing

that distance-based ABC can approach optimal classification even without explicitly sufficient summaries. For $n = 1000$, all ABC-based methods correctly identified the true model in every case, and we therefore omit the results.

ABC-SA performs worse than ABC-Stat, likely due to its reliance on general-purpose summary statistics rather than sufficient problem-specific sufficient summaries, available in this specific case.

ABC-QDA shows variable performance across ABC methods, with correct model selection probabilities below 90% for simulations from M_2 and M_3 . Its reliance on QDA to separate observed and simulated data, followed by selection of simulations with low classification accuracy, appears better suited to parameter inference than model choice. Under misspecification, incorrect models can closely mimic the true model (Berk, 1966), and a possible explanation of ABC-QDA behavior is that the estimation process concentrates to parameter values that make the model closer to the true one, leading to lower classification accuracy and higher MSE for parameter estimates.

NN is the method that show the lowest accuracy of model selection: it correctly identifies the exponential model in only 78% of cases, the lognormal in 81%, and the gamma in around 20%. The gamma model was often misclassified as exponential, suggesting a structural limitation in distinguishing these distributions.

Parameter estimation results (Table 2) mirror these findings. For distance-based ABC methods, MSEs are consistently low when the correct model is selected, comparable to ABC-Stat. By contrast, NN produces biased estimates, reflecting its difficulty in identifying the correct model. ABC-SA yields slightly higher estimation errors. Finally, ABC-QDA has the largest MSE values across all experiments and ABC methods.

		ABC						NN	ABC	
		CvM	MMD	MMD (log)	Wass	Wass (log)	Stat		SA	QDA
$\mathcal{E}\text{xp}(0.5)$	$\Pr(M = M_1)$	0.883	0.836	0.953	0.850	0.948	0.952	0.775	0.772	0.922
	$\hat{\theta}$	0.512	0.506	0.511	0.515	0.514	0.513	10.424	0.510	0.522
	MSE	0.003	0.003	0.003	0.003	0.003	0.003	102.712	0.003	0.0040
$\mathcal{LN}(0.193, 1)$	$\Pr(M = M_2)$	0.896	0.829	0.952	0.882	0.956	0.954	0.810	0.787	0.875
	$\hat{\theta}$	0.188	0.196	0.187	0.189	0.187	0.191	10.747	0.204	0.187
	MSE	0.009	0.008	0.008	0.008	0.009	0.010	108.699	0.013	0.140
$\mathcal{Ga}(2, 1)$	$\Pr(M = M_3)$	0.952	0.966	0.971	0.984	0.987	0.987	0.175	0.955	0.819
	$\hat{\theta}$	1.000	0.995	0.998	1.004	1.003	1.002	10.789	1.017	1.000
	MSE	0.004	0.004	0.004	0.004	0.004	0.004	108.416	0.008	0.275

TABLE 2

Results for the exponential family models across repetitions. For each model, we report the average posterior probability of selecting the correct model, the average estimate of the parameter θ , and the MSE across repetitions.

4.2.1. Computational Performance Comparison

The proposed approaches exhibit varying computational costs. For both NN and ABC methods, we generated 10^6 datasets, resulting in similar training times.

For $n = 100$, the computation times for distance calculations between one observed dataset and one simulated dataset are approximately 0.0018 s for ABC-CvM, 0.0001 s for ABC-Wass, and 0.2685 s for ABC-MMD. For $n = 1000$, the times are approximately 0.0040 s for ABC-CvM, 0.0013 s for ABC-Wass, and 0.2738 s for ABC-MMD. Hence, ABC-MMD is the most computationally demanding, with running times more than 2,000 times slower than ABC-Wass and almost 150 times slower than ABC-CvM. This is because standard MMD computation requires pairwise kernel evaluations between all points in both datasets, resulting in $\mathcal{O}(n^2)$ complexity. In contrast, metrics like the Wasserstein distance can often be computed more efficiently, especially in one dimension. Moreover, MMD relies on kernel functions mapping data into a reproducing kernel Hilbert space (RKHS), adding further computational burden. For comparison, ABC-QDA (Gutmann et al., 2018) takes 0.0529 s to perform QDA on the observed and simulated datasets, making it more computationally demanding than ABC-CvM and ABC-Wass.

Total runtime depends on available computational resources. In our example, the analyses were executed in parallel on a 24-core Intel Xeon Scalable ‘Cascade Lake’ processor with 8.91 GB of DDR4 RAM. Processing 100 observed datasets, each compared against 10^6 simulated datasets using six distance metrics, took approximately one hour. By contrast, the deep neural network with 5 layers required 256 s to train over 10 epochs and an additional 4 s for testing.

Subsequent examples show comparable computational times, so we omit further runtime comparisons.

4.3. *g-and-k Distribution Model Selection*

Being a standard benchmark in the ABC literature for problems with intractable likelihoods, we consider a model selection problem involving the *g-and-k* distribution (Rayner and MacGillivray, 2002). This distribution is defined via its quantile function:

$$\mathcal{Q}(p; a, b, c, g, k) = a + b \left(1 + c \frac{1 - e^{-gz(p)}}{1 + e^{-gz(p)}} \right) \cdot (1 + z(p)^2)^k z(p),$$

where $z(p)$ denotes the quantile function of the standard normal distribution. The constant $c = 0.8$ ensures that \mathcal{Q} defines a proper distribution. Parameters $a, b > 0$ represent location and scale, g controls skewness, and $k > -\frac{1}{2}$ controls kurtosis. The *g-and-k* distribution is attractive for its flexibility, but the absence of a closed-form density complicates standard likelihood-based inference.

Following Marin et al. (2013), we fix $a = 0$, $b = 1$, and $c = 0.8$, and focus on model selection between two submodels: M_1 : $g = 0$ (no skewness) vs M_2 : $g \neq 0$ with $g \sim U(0, 4)$ (positive skewness). We treat k as unknown under both models, with prior $k \sim U(-0.5, 5)$. Thus, the task reduces to a hypothesis test for skewness in the presence of unknown kurtosis.

Observed datasets are simulated using $g = 0$, $k = 2$ under M_1 and $g = 1$, $k = 2$ under M_2 , following Marin et al. (2013). These parameter settings yield

models that produce similar data distributions, making classification deliberately challenging. Appendix F in the Supplementary Material illustrates the overlap between the distributions under M_1 and M_2 .

In the ABC-Stat method, following Marin et al. (2013), the 0.1 and 0.9 quantiles are used as summary statistics, and the L_1 distance is employed. This choice is theoretically justified to recover the correct model asymptotically under both M_1 and M_2 . All reported results based on ABC methods use the 0.1% acceptance threshold. Since the observations can be negative, log-transformations are not feasible, and distances are therefore computed on the untransformed data.

Tables 3 and 4, and Appendix F in the Supplementary Material present results for this example, for sample sizes $n = 100$ and $n = 1000$. For $n = 100$ and when M_1 is the true model, full data ABC methods yield an average estimated probability around 0.80, which increases to 0.90 when the sample size grows to $n = 1000$. ABC-MMD performs slightly worse than the other methods, particularly for the larger sample size, where it still show high variability (see boxplots in the Supplementary Material).

When the data are generated from M_2 , the estimated probabilities for $n = 100$ are lower and varying depending on the method, but they approach one as $n = 1000$, with the exception of ABC-MMD. Overall, ABC-Wass outperforms the other methods, producing consistently higher estimates of the posterior probability of the correct model and converging to one more quickly as the sample size increases, indicating strong discriminative performance.

These results are supported by the confusion matrices in Appendix F of the Supplementary Material, which show that ABC methods based on distance metrics outperform the alternatives. Among them, ABC-Wass achieves the strongest performance, reaching near-perfect classification when $n = 1000$.

By contrast, NN consistently underperforms. Even for large sample sizes, it tends to assign higher posterior probability to M_1 , leading to frequent misclassification of data generated under M_2 . This indicates that standard neural network architectures may not be well-suited for subtle model discrimination tasks without careful tuning or domain-specific design.

The behavior of ABC-SA is apparently surprising. At $n = 100$, its performance is comparable to full data ABC methods, but when $n = 1000$ it systematically favors M_1 even when the data arise from M_2 . However, to reduce dimensionality and memory usage in this case, only every fifth order statistic was retained at $n = 1000$ as initial vector of statistics, which may have limited the discriminative power of the summaries. This factor likely explains the counterintuitive misclassification pattern: the summary statistics provided to the semi-automatic procedure are less representative of the sample.

ABC-QDA performs poorly across all scenarios, with high variability in the estimated posterior probabilities. This behavior reflects its sensitivity to model misspecification, whereby parameters from an incorrect model can approximate the data closely enough to obscure clear classification boundaries; this behavior is also suggested by the estimated values of g shown in Tables 3 and 4, which are associated with the largest MSEs.

Although some methods achieve strong classification performance, this does

not always translate into accurate parameter recovery. For example, while ABC-Wass is highly effective for model selection, it is known to perform less well when estimating parameters under the g -and- k model (Drovandi and Frazier, 2022), where ABC-CvM provides more accurate parameter inference. This pattern is confirmed in Tables 3 and 4, which show that the MSE for estimating g tends to be lower for ABC-CvM than ABC-Wass.

NN struggles to estimate the g parameter, producing highly variable estimates that misleadingly suggest negative skewness. ABC-SA yields estimates comparable to other ABC methods under M_1 , but systematically underestimates g under M_2 . In contrast, ABC-QDA tends to produce similar estimates for g across models M_1 and M_2 , reducing its ability to distinguish between them.

Across all scenarios, all methods show improved performance when estimating the k parameter.

		ABC				NN	ABC	
		CvM	MMD	Wass	Stat		SA	QDA
$g = 0.0$	$\Pr(M = M_1)$	0.793	0.701	0.808	0.788	0.993	0.774	0.582
	\hat{g}	0.164	0.342	0.291	0.262	-10.288	0.190	1.533
	MSE (g)	0.308	0.712	0.540	0.508	177.849	0.229	2.516
	\hat{k}	2.018	2.001	1.995	2.009	1.560	2.015	2.016
	MSE (k)	0.074	0.089	0.048	0.118	2.213	0.077	0.171
$g = 1.0$	$\Pr(M = M_2)$	0.735	0.656	0.832	0.742	0.010	0.846	0.475
	\hat{g}	1.163	0.825	1.103	1.205	-12.322	0.678	1.738
	MSE (g)	0.890	1.035	1.127	1.086	468.111	0.460	0.734
	\hat{k}	2.066	1.954	2.005	2.040	1.454	3.759	2.131
	MSE (k)	0.089	0.104	0.051	0.133	2.730	3.112	0.265

TABLE 3

Results for datasets of size $n = 100$ generated from a g -and- k distribution with unknown g and k . For each model ($g = 0$ and $g \neq 0$), we report the average posterior probability of the correct model, the average posterior means of g and k , and their mean squared errors (MSE).

		ABC				NN	ABC	
		CvM	MMD	Wass	Stat		SA	QDA
$g = 0.0$	$\Pr(M = M_1)$	0.930	0.844	0.942	0.914	0.858	0.895	0.614
	\hat{g}	0.000	0.025	0.000	0.000	-4.994	0.000	1.308
	MSE (g)	0.000	0.020	0.000	0.000	198.506	0.000	1.933
	\hat{k}	2.010	2.013	1.988	2.009	1.998	1.975	1.880
	MSE (k)	0.007	0.008	0.004	0.010	0.003	0.011	0.041
$g = 1.0$	$\Pr(M = M_2)$	0.991	0.775	0.999	0.981	0.210	0.152	0.386
	\hat{g}	1.012	0.955	1.2301	1.034	-3.005	0.040	1.518
	MSE (g)	0.044	0.210	0.166	0.077	80.471	0.946	0.645
	\hat{k}	2.027	2.018	1.988	2.008	2.001	1.833	2.010
	MSE (k)	0.010	0.013	0.008	0.014	0.004	0.052	0.046

TABLE 4

Results for datasets of size $n = 1000$ generated from a g -and- k distribution with unknown g and k . For each model ($g = 0$ and $g \neq 0$), we report the average posterior probability of the correct model, the average posterior means of g and k , and their mean squared errors (MSE).

4.4. Toad Movement Model Selection

Toads exhibit a strong tendency to return to previously visited sites while occasionally making long-distance moves. This behavior aligns well with the multiscaled random walk (MRW) model introduced by [Gautestad and Mysterud \(2005\)](#), which incorporates a power-law step distribution. Unlike memory-free random walks such as Lévy flights ([Viswanathan et al., 1999](#); [Humphries et al., 2010](#); [Sims et al., 2014](#)), the MRW accounts for return steps and models the development of a cognitive map, leading to non-random spatial reuse. Although power-law models are flexible, a key challenge remains in effectively capturing return behavior, which is crucial for understanding amphibian movement.

Following [Marchand et al. \(2017\)](#), the random return step for toads occurs at the end of their nighttime foraging journey, when they perform a displacement S_n from their last refuge location Y_n . The toad either moves to a new location, $Y_{n+1} = Y_n + S_n$, or returns to a previous daytime refuge site (Y_i for some $i = 1, \dots, n-1$). Under the MRW, the displacement follows a symmetric, zero-centered stable distribution, $S_n \sim S(\alpha, \gamma)$, defined via its characteristic function

$$\varphi(t; \alpha, \gamma) = e^{-|\gamma t|^\alpha},$$

where $0 \leq \alpha \leq 2$ is a stability parameter and $\gamma > 0$ is a scale parameter. Decreasing values of α lead to increasingly leptokurtic distributions, allowing rare long-distance events to be effectively modeled, which is ideal for capturing toad movements. Notably, the probability density function of this family is intractable, as it is given by the inverse Fourier transform of the characteristic function.

Despite the intractable density, $S(\alpha, \gamma)$ can be sampled using the CMS algorithm ([Chambers et al., 1976](#)), enabling posterior inference via ABC. We consider three candidate models for toad return behavior. For each model, the toad starts at $Y_1 = 0$, and the step sizes $S_n \sim S(\alpha, \gamma)$ are i.i.d. for $n = 1, \dots, d-1$. Individual toads are assumed to behave independently.

Model M_1 is the random return model, which assumes a constant probability of return, p_0 , for the toad to any previously visited site. The return site is chosen randomly from all prior sites. Locations that have been visited multiple times naturally have higher chances of being revisited, allowing home range patterns to emerge. Under Model M_1 , the random refuge location at the beginning of day $(n+1) \in \{2, \dots, n_d\}$ is given by

$$Y_{n+1} = \begin{cases} Y_n + S_n & \text{with prob. } 1 - p_0, \\ Y_i & \text{with prob. } p_0/n \quad \forall i = 1, \dots, n. \end{cases}$$

Model M_2 also uses a constant probability of return p_0 but incorporates distance by assuming that, when the toad returns, it always chooses the nearest refuge site. Formally:

$$Y_{n+1} = \begin{cases} Y_n + S_n & \text{with prob. } 1 - p_0, \\ \min_{Y \in \{Y_1, \dots, Y_n\}} |Y_{n+1} - Y| & \text{with prob. } p_0. \end{cases}$$

Model M_3 is a distance-based return model, where the probability of returning to a given site i decays exponentially with the distance d_i from that refuge: $p_{ret(i)} = p_0 e^{-d_i/d_0}$, with d_0 controlling the strenght of the distance effect. Let A_n denote the number of unique previous refuge sites at day n , R_1, \dots, R_{A_n} , such that $R_i \neq R_j \forall i \neq j$ and each $R_i = Y_j$ for some $j \in \{1, \dots, n-1\}$. Multiple visits to the same location do not create new refuge sites. Assuming independence between previous sites, the movement model is

$$Y_{n+1} = \begin{cases} Y_n + S_n & \text{with prob. } \prod_{j=1}^{A_{n+1}} (1 - p_{ret(j)}), \\ R_i & \text{with prob. } p_i \quad \forall i = 1, \dots, A_{n+1}, \end{cases}$$

where

$$p_i = \frac{p_{ret(i)}}{\sum_{j=1}^{A_{n+1}} p_{ret(j)}} \left(1 - \prod_{j=1}^{A_{n+1}} (1 - p_{ret(j)}) \right).$$

If $Y_{n+1} = Y_n + S_n$, a new refuge site is created and $A_{n+2} = A_{n+1} + 1$; otherwise $A_{n+2} = A_{n+1}$.

For the ABC model selection procedure, given the higher computational burden of the simulation, we generated only 10^5 simulated datasets, assuming a uniform prior over the three models. Parameter priors follow [Marchand et al. \(2017\)](#): $\alpha \sim U(1, 2)$, $\gamma \sim U(10, 100)$, $p_0 \sim U(0, 1)$, and $d_0 \sim U(20, 2000)$.

To reduce the dimensionality of the observed data, we summarise it as follows. For a set of time lags $\ell = 1, 2, 4, 8$, we compute displacements $\mathbf{y}_\ell = \{|\mathbf{y}_{i+\ell, j} - \mathbf{y}_{i, j}| \mid 1 \leq i \leq n_d - \ell, 1 \leq j \leq n_t\}$. Returns are defined as displacements smaller than 10 meters, i.e. $|\{x \in \mathbf{y}_\ell \mid x \leq 10\}|$, and non-returns are displacements greater than or equal to 10 meters. For each lag, we extract 12 summary statistics: the return count and the 11 log-differences of deciles (quantiles at 0.0, 0.1, ..., 1.0) of the non-return distances (including the median). Across four lags, the resulting summary vector has 48 elements. Edge cases (e.g. no non-return events or zero quantile differences) are handled using missing values to avoid computational issues. This construction can be regarded as a hybrid approach, since the observed dataset is not used directly but is instead represented by a set of carefully designed summary statistics that combine return counts with decile-based quantile differences of non-return distances.

We propose a weighted distance metric that combines normalized return-count distances and statistical distances on non-return displacements across lags. Let $\mathcal{D}_1^{(i)}, \dots, \mathcal{D}_8^{(i)}$ be the distances for the i -th simulated dataset, where $\mathcal{D}_{1:4}^{(i)}$ correspond to return counts and $\mathcal{D}_{5:8}^{(i)}$ correspond to statistical distances of non-return displacements at each lag. The combined distance is defined as:

$$\mathcal{D}^{(i)} = \omega \frac{\sum_{k=1}^4 \mathcal{D}_k^{(i)}}{\max_{j=1, \dots, N} \sum_{k=1}^4 \mathcal{D}_k^{(j)}} + (1 - \omega) \frac{\sum_{k=5}^8 \mathcal{D}_k^{(i)}}{\max_{j=1, \dots, N} \sum_{k=5}^8 \mathcal{D}_k^{(j)}} \quad \omega \in [0, 1].$$

Simulation experiments indicated that lower weights on the return-count component ($\omega \leq 0.2$) yielded more accurate model recovery, suggesting that fine-

grained information in the non-return displacements is more informative than return counts alone. All results reported below use $\omega = 0.2$.

As a benchmark, we also implemented the ABC-Stat method from [Drovandi and Frazier \(2022\)](#), using the same 48 summary statistics and a weighted Euclidean distance. The weights are given by the reciprocal of the median absolute deviation (MAD) of the prior predictive distribution for each statistic ([Prangle, 2017](#)). Given observed data show skewness, we implemented ABC-MMD and ABC-Wass with both untransformed data and log-transformed data.

To assess model recovery, we generated 100 datasets from each model using the parameter values in [Marchand et al. \(2017\)](#): $(\alpha, \gamma, p_0) = (1.7, 34, 0.6)$ for M_1 , $(\alpha, \gamma, p_0) = (1.83, 46, 0.65)$ for M_2 , and $(\alpha, \gamma, p_0, d_0) = (1.65, 32, 0.43, 758)$ for M_3 . Each simulated dataset mirrors the structure of the real data used in Section 5, with $n_t = 66$ individuals observed over $n_d = 63$ days.

Table 5 summarizes the posterior model probabilities across 100 datasets for each method, and Appendix G includes the corresponding confusion matrices and boxplots. ABC-Wass (log) consistently exhibits the highest mean posterior probabilities for the correct models, regardless of which model generated the data. Boxplots in Appendix G further indicate tight interquartile ranges, reflecting consistent performance across replicates. ABC-CvM and ABC-MMD (log) also perform well, although ABC-MMD (log) shows slightly more variability and lower mean probabilities compared to ABC-Wass (log). Overall, Model M_2 is the most easily recognizable, while Models M_1 and M_3 display more variable classification depending on the method.

ABC-Stat demonstrates good performance, with mean posterior probabilities around 0.70–0.75 for Models M_1 and M_3 , and higher for Model M_2 , similar to ABC-CvM and ABC-MMD. Parameter estimation is also similar to other methods.

NN exhibits lower classification accuracy across all models, with mean posterior probabilities close to 0.50, indicating near-random performance. Parameter estimation is also poor, with high variability. This may be an indication of a tendency to overfit, so that similar models are less easy to identify. Again, Model M_2 shows a higher average posterior probability (around 0.80), although still lower with respect to other methods.

ABC-SA, as implemented in the `abctools` R package, encountered memory limitations; to mitigate this, the number of summary statistics was reduced from 48 to 20. This likely contributed to its decreased performance relative to ABC-Stat. Model M_2 remains relatively easy to identify, with an average posterior probability larger than 0.95, but Models M_1 and M_3 are frequently misclassified. Parameter estimation under ABC-SA remains competitive with respect to the other methods.

ABC-QDA generally follows the overall structure of the ABC methods but shows lower classification accuracy, particularly for Model M_1 , which is often misclassified as Model M_3 , and viceversa. Parameter estimation is similarly affected, with the highest MSE values, together with NN. This may be an indication that wrong models are estimated as closely as possible to the correct model.

Overall, these results highlight the importance of carefully selecting the distance metric and considering appropriate data transformations. Among all methods, ABC-Wass (log) provides the best performance in model selection, combining high posterior probabilities with low variability, and demonstrates competitive reliability for parameter estimation when models are correctly identified.

		ABC					Stat	NN	ABC	
		CvM	MMD	MMD (log)	Wass	Wass (log)			SA	QDA
M_1	$\Pr(M = M_1)$	0.711	0.714	0.802	0.784	0.926	0.741	0.471	0.632	0.478
	$\hat{\alpha}$	1.732	1.796	1.778	1.703	1.687	1.772	1.598	1.748	1.811
	MSE_α	0.012	0.027	0.022	0.003	0.001	0.014	0.052	0.021	0.030
	$\hat{\gamma}$	34.891	38.232	36.682	34.193	33.877	35.511	29.298	36.096	38.701
	MSE_γ	8.198	35.123	20.877	2.602	2.089	12.023	46.179	19.598	41.278
	\hat{p}_0	0.609	0.657	0.648	0.602	0.587	0.638	0.523	0.619	0.667
	MSE_{p_0}	0.004	0.011	0.008	0.002	0.001	0.006	0.020	0.009	0.013
M_2	$\Pr(M = M_2)$	0.958	0.918	0.968	0.951	0.989	0.957	0.781	0.962	0.881
	$\hat{\alpha}$	1.841	1.898	1.882	1.829	1.822	1.869	1.701	1.861	1.908
	MSE_α	0.009	0.023	0.019	0.003	0.001	0.013	0.048	0.018	0.032
	$\hat{\gamma}$	45.179	48.088	47.289	45.912	45.783	46.223	39.121	46.978	49.003
	MSE_γ	6.498	31.975	20.092	2.797	2.011	11.401	50.876	18.889	43.472
	\hat{p}_0	0.638	0.691	0.677	0.653	0.641	0.672	0.581	0.661	0.698
	MSE_{p_0}	0.005	0.012	0.009	0.002	0.001	0.007	0.018	0.007	0.015
M_3	$\Pr(M = M_3)$	0.701	0.719	0.881	0.732	0.909	0.738	0.458	0.652	0.501
	$\hat{\alpha}$	1.659	1.698	1.682	1.641	1.652	1.689	1.599	1.669	1.709
	MSE_α	0.006	0.020	0.015	0.002	0.001	0.010	0.041	0.016	0.026
	$\hat{\gamma}$	32.603	34.514	33.278	32.296	32.111	33.821	28.003	33.998	35.124
	MSE_γ	4.102	30.178	17.867	2.201	1.723	9.312	48.523	16.012	39.563
	\hat{p}_0	0.438	0.482	0.459	0.428	0.432	0.458	0.392	0.451	0.498
	MSE_{p_0}	0.003	0.010	0.007	0.001	0.001	0.006	0.014	0.007	0.011
	\hat{d}_0	762	785	770	757	758	773	710	769	800
	MSE_{d_0}	8.598	32.421	19.289	2.503	1.893	10.504	49.689	21.179	44.120

TABLE 5

Results for the toad movement example across 100 repetitions. For each method, the probability of selecting the correct model $\Pr(M = M_i)$, the posterior mean of the parameters for the selected model, and the corresponding MSEs are shown.

5. Real Data Example

The data were collected on the north shore of Lake Erie in Ontario, Canada, and consist of daytime and nighttime location recordings of Fowler's toads inhabiting a linear sand dune habitat. Toads were fitted with radiotransmitters between mid-June and late August in both 2009 and 2010. Each individual's location was recorded at least once per night while foraging and once per day while resting in a refuge. For the present analysis, only the daytime recordings are used, as they provide information most relevant to the toads' return behavior. In total, $n_t = 66$ toads were tracked over $n_d = 63$ days.

To simplify analysis, the two-dimensional (northing and easting) location data were projected onto a one-dimensional axis parallel to the shoreline. This projection removes variation orthogonal to the shoreline that is influenced by

ecological factors (e.g., wave action or predator avoidance) but not directly related to return behavior. By contrast, movement along the shoreline is largely unconstrained. This transformation yields an $n_d \times n_t$ observation matrix, where each entry represents the projected one-dimensional location of a toad on a given day. The dataset is publicly available at: <https://github.com/pmarchand1/fowlers-toad-move/>

We use the same summary statistics defined in Section 4.4, which describe both the return and non-return data, resulting in a total of 48 summary statistics that form the low-dimensional observed dataset. Step distributions of the non-return data are shown in Figure 2. These distributions exhibit strong positive skewness and a heavy right tail at each lag. Such features motivate the use of log-transformations when applying full data ABC approaches (in particular, for ABC-MMD and ABC-Wass).

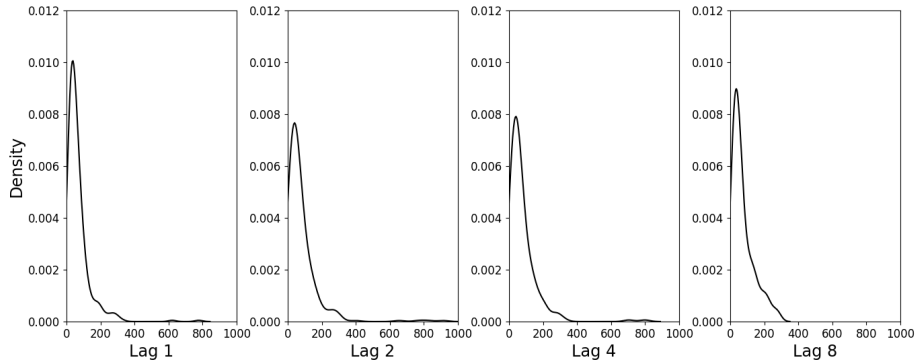


Figure 2: Kernel density estimates of the non-return data across different lags, based on the real observations.

The estimated posterior probabilities for each model and method are reported in Table 6 together with the original results from Marchand et al. (2017). Across all methods, the highest posterior probability is assigned to the distance-based return model M_3 , indicating consistent support for this model across the ABC approaches implemented here, the original study, and the competitors. Notably, ABC-CvM, ABC-MMD (log), and ABC-Wass (log) allocate higher posterior mass to M_3 compared with the original findings, with ABC-Wass (log) assigning full support to the distance-based model. By contrast, ABC-MMD, ABC-Stat, NN, and ABC-SA provide weaker support for M_3 , with moderate probability also assigned to M_1 . All methods consistently assign zero (or near-zero) posterior probability to M_2 .

It is noteworthy that the full data approaches assign posterior probabilities to M_3 that exceed the highest values observed for simulated datasets generated under M_3 (Table 5 of Section 4.4). One interpretation is that model misspecification inflates support for M_3 while reducing support for the alternatives. This

	$\Pr(M = M_1)$	$\Pr(M = M_2)$	$\Pr(M = M_3)$
ABC-CvM	0.08	0.00	0.92
ABC-MMD	0.29	0.00	0.71
ABC-MMD (log)	0.07	0.00	0.93
ABC-Wass	0.14	0.00	0.86
ABC-Wass (log)	0.00	0.00	1.00
ABC-Stat	0.40	0.00	0.60
ABC-Stat (Marchand et al., 2017)	0.15	0.00	0.85
NN	0.32	0.02	0.66
ABC-SA	0.36	0.00	0.64
ABC-QDA	0.13	0.09	0.79

TABLE 6

Estimated posterior probabilities of the three toad movement models, comparing different methods with the original results of Marchand et al. (2017).

aligns with the view that distance-based ABC methods tend to be robust to misspecification in parameter inference (Frazier, 2020; Legramanti et al., 2025), as also suggested by Theorem 3.2.

These results also reproduce the main results of Marchand et al. (2017), but not their final conclusion that M_1 was most suitable. That conclusion was shaped by the limited performance of their ABC approach on simulated data, where high posterior error rates occurred for datasets from both M_1 and M_3 . To address this, the authors supplemented their analysis with an external comparison of refuge site numbers, which favoured M_1 . In contrast, the full data methods proposed here show strong performance in simulation (Section 4.4), reliably recovering the true model. While ABC-MMD, ABC-Wass, ABC-Stat, ABC-SA, and ABC-QDA perform reasonably well, they display greater uncertainty than ABC-CvM, ABC-MMD (log), and ABC-Wass (log), which are the methods providing the largest support to M_3 .

Taken together, our results suggest that the distance-based return model M_3 provides a more consistent explanation of the observed data than the alternatives within the set of models considered. In particular, M_3 implies that rare long-distance movements are unlikely to result in a return to previous sites. This contrasts with M_1 (random return) and M_2 (nearest return), where the return probability remains constant at p_0 regardless of distance. The stronger support for M_3 therefore highlights a potentially more intuitive and ecologically plausible mechanism: new refuges may be more likely to be established when a toad is far from prior locations. These interpretations should be viewed with caution, however, as no formal goodness-of-fit assessment was performed.

In terms of parameter estimation (Figure 3), all methods provide accurate estimates for the return strength parameter α , with consistently low variability across methods. Greater uncertainty is observed for γ , p_0 , and d_0 , particularly under ABC-MMD, ABC-Wass, NN, and ABC-QDA. Among these, NN exhibits the highest uncertainty, likely due to difficulties in identifying the correct model. Overall, these results suggest that once the correct model is identified, distance-based ABC methods yield reliable parameter estimates.

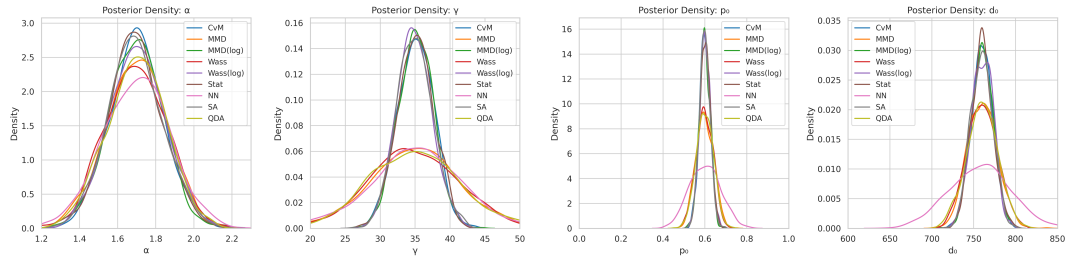


Figure 3: Posterior distributions of model M_3 parameters across the considered methods.

6. Conclusion

This work has investigated ABC as a tool for model selection in settings with intractable likelihoods. While ABC is well established for parameter inference, model selection remains challenging, largely due to sensitivity to the choice of summary statistics. Insufficient statistics can lead to severe information loss and unreliable model choice.

Our primary contribution is an empirical evaluation of ABC model selection using statistical distances computed on the full data, avoiding summary statistics altogether. Extensive simulation studies demonstrate that full data ABC approaches yield posterior distributions closely matching ABC with sufficient statistics (when they are sufficient for model choice problems as in Section 4.1 and 4.2) or provides high support to the correct model (Section 4.3 and 4.4), suggesting that statistical distances preserve key data features necessary for accurate model comparison. Given that sufficient statistics are rarely available in complex applications, full data ABC offers a robust alternative for likelihood-free model selection.

Across all simulations, the Wasserstein distance consistently produced the most accurate model selection results, achieving near-exact posterior approximations, faster convergence to the true model, and lower misclassification rates. The Cramér–von Mises distance and the Maximum Mean Discrepancy also performed well in simpler settings, but their effectiveness varied with sample size and model complexity. In some cases, data transformations were necessary to ensure robust performance under asymmetric distributions, echoing previous findings in parameter estimation contexts (Drovandi and Frazier, 2022).

The theoretical results presented in Section 3 establish both the consistency of ABC-Wass in selecting the correct model (Theorem 3.1) and its robustness to model misspecification (Theorem 3.2), i.e. when the true data-generating model is not included in the candidate class. These results highlight an important advantage: the assumptions required are mild and easily verifiable, particularly in the common case of i.i.d. data. Moreover, our simulation studies on non-i.i.d. observations suggest that the Wasserstein distance retains its good performance

in practice, further supporting its applicability beyond the theoretical setting. Since sufficient statistics are rarely available in the complex scenarios where ABC is typically applied, and the use of insufficient summaries can induce unbounded information loss (Robert et al., 2011), our findings underscore the potential of full data ABC approaches based on Wasserstein distance. These methods provide a principled and reliable foundation for model selection in likelihood-free inference, balancing both theoretical guarantees and empirical performance. Future work will extend these results by leveraging the general framework of Legramanti et al. (2025), which accommodates a range of statistical distances and thus provides a natural platform for validating discrepancy-based ABC under broader conditions.

In the toad movement case study, full data ABC approaches both confirmed and refined earlier conclusions: the distance-based return model received the highest posterior support, contrasting with the random return model previously favored by Marchand et al. (2017). Their conclusion relied heavily on visual inspection of model fit for simulated data, whereas model classification performed better under the distance-based ABC methods applied here. This analysis demonstrates that ABC using statistical distances is both consistent and interpretable, providing ecologically plausible insights while reliably distinguishing competing models. Parameter estimation further corroborated these findings, with lower variability observed for methods that performed well in model selection.

While this study employed the standard rejection ABC algorithm to enable fair comparisons across distance metrics, integrating statistical distances into more efficient ABC schemes (Toni and Stumpf, 2010; Didelot et al., 2011) represents a natural next step, particularly in settings where computational cost is critical. Rejection ABC also allows full parallelisation, which we leveraged in our computational performance evaluations. Although more advanced ABC algorithms may improve efficiency, we do not expect them to substantially alter the comparative performance of the distance metrics.

Although full data ABC methods avoid low-dimensional summary statistics, they remain subject to the curse of dimensionality: Wasserstein distances grow exponentially with dimension (Fournier and Guillin, 2015; Bernton et al., 2019), and MMD may lose power due to kernel sensitivity (Ramdas et al., 2015). Effective application therefore requires careful choice of distance metric and strategies to manage computational complexity, such as dimensionality reduction, adaptive weighting, or feature learning. In other words, full data ABC does not eliminate the curse of dimensionality, it shifts the challenge, requiring practitioners to regularize the discrepancy measure and manage high-dimensional effects.

In summary, our findings demonstrate that ABC with statistical distances offers a promising framework for likelihood-free model selection. These methods provide accurate, interpretable results, reduce reliance on summary statistics, and perform robustly under realistic model misspecification. They may also motivate a re-evaluation of past ABC analyses that relied on potentially insufficient summaries, paving the way toward a more problem-invariant and reliable ABC methodology for Bayesian model selection in complex statistical models.

Appendix A: ABC algorithms

This Appendix presents two rejection ABC algorithms used for parameter inference and one used for model selection.

Algorithms 2 and 3 are aimed at statistical inference. Algorithm 2 makes use of summary statistics, while Algorithm 3 makes use of statistical distances. Algorithm 4 performs model selection using summary statistics and it has been shown to be inconsistent in most cases by Robert et al. (2011).

Algorithm 2 Summary-based ABC

- 1: **Input:** Given a set of observations $\mathbf{y} = (y_1, \dots, y_n)^T$, an observed summary statistics $\boldsymbol{\eta}(\mathbf{y})$, a tolerance level ε , and a distance $\rho(\cdot, \cdot)$:
 - 2: **for** $i = 1, \dots, N$ **do**
 - 3: **repeat**
 - 4: Generate $\boldsymbol{\theta}^*$ from $\pi(\boldsymbol{\theta})$.
 - 5: Generate $\mathbf{z} = (z_1, z_2, \dots, z_n)^T$ from $P_{\boldsymbol{\theta}^*}^{(n)}$.
 - 6: **until** $\rho(\boldsymbol{\eta}(\mathbf{y}), \boldsymbol{\eta}(\mathbf{z})) \leq \varepsilon$
 - 7: Set $\boldsymbol{\theta}^{(i)} = \boldsymbol{\theta}^*$.
 - 8: **end for**
 - 9: **Output:** A set of values $(\boldsymbol{\theta}^{(1)}, \dots, \boldsymbol{\theta}^{(N)})$ from $\pi_\varepsilon(\boldsymbol{\theta}|\boldsymbol{\eta}(\mathbf{y}))$.
-

Algorithm 3 Discrepancy-based ABC

- 1: **Input:** Given a set of observations $\mathbf{y} = (y_1, \dots, y_n)^T$, a tolerance level ε , and a discrepancy metric $\mathcal{D}(\cdot, \cdot)$:
 - 2: **for** $i = 1, \dots, N$ **do**
 - 3: **repeat**
 - 4: Generate $\boldsymbol{\theta}^*$ from $\pi(\boldsymbol{\theta})$.
 - 5: Generate $\mathbf{z} = (z_1, z_2, \dots, z_n)^T$ from $P_{\boldsymbol{\theta}^*}^{(n)}$.
 - 6: **until** $\mathcal{D}(\hat{\mu}_{\boldsymbol{\theta}_0}, \hat{\mu}_{\boldsymbol{\theta}^*}) \leq \varepsilon$
 - 7: Set $\boldsymbol{\theta}^{(i)} = \boldsymbol{\theta}^*$.
 - 8: **end for**
 - 9: **Output:** A set of values $(\boldsymbol{\theta}^{(1)}, \dots, \boldsymbol{\theta}^{(N)})$ from $\pi_\varepsilon(\boldsymbol{\theta}|\mathbf{y})$.
-

Algorithm 4 Summary-based ABC-MC

1: **Input:** Given a set of observations $\mathbf{y} = (y_1, \dots, y_n)^T$, a set of possible models $\{M_1, M_2, \dots, M_K\}$, an observed summary statistics $\boldsymbol{\eta}(\mathbf{y})$, a tolerance level ε , and a distance $\rho(\cdot, \cdot)$;
2: **for** $i = 1, \dots, N$ **do**
3: **repeat**
4: Generate M_{k^*} from $\pi(M_k)$, $k = 1, \dots, K$.
5: Generate $\boldsymbol{\theta}_{k^*}$ from $\pi_{k^*}(\boldsymbol{\theta}_{k^*})$.
6: Generate $\mathbf{z} = (z_1, \dots, z_n)^T$ from $P_{M_{k^*}, \boldsymbol{\theta}_{k^*}}^{(n)}$.
7: **until** $\rho(\boldsymbol{\eta}(\mathbf{y}), \boldsymbol{\eta}(\mathbf{z})) \leq \varepsilon$,
8: Set $M^{(i)} = M_{k^*}$ and $\boldsymbol{\theta}^{(i)} = \boldsymbol{\theta}_{k^*}$.
9: **end for**
10: **Output:** A set of values $(M^{(1)}, \dots, M^{(N)})$ and $(\boldsymbol{\theta}^{(1)}, \dots, \boldsymbol{\theta}^{(N)})$ from $\pi_\varepsilon(M_k | \boldsymbol{\eta}(\mathbf{y}))$ and $\pi_{\varepsilon, k}(\boldsymbol{\theta}_k | \boldsymbol{\eta}(\mathbf{y}), M_k)$, for $k = 1, \dots, K$, respectively.

Appendix B: Proof of Theorem 3.1

Proof. Let the observed data \mathbf{y} be i.i.d. from $P_{M_0, \boldsymbol{\theta}_0}^{(n)}$. For a candidate model M_{k^*} with parameter $\boldsymbol{\theta}_{k^*} \in \Theta_{k^*}$ denote the population law by $P_{M_{k^*}, \boldsymbol{\theta}_{k^*}}^{(n)}$. Define the ABC numerator for model M_{k^*} with threshold ε_n by

$$N_{k^*}(n) := \pi(M_{k^*}) \int_{\Theta_{k^*}} \pi_{M_{k^*}}(\boldsymbol{\theta}_{k^*}) \mathbb{P}(\mathcal{W}_p(\hat{\mu}_0, \boldsymbol{\theta}_0, \hat{\mu}_{k^*}, \boldsymbol{\theta}_{k^*}) \leq \varepsilon_n) d\boldsymbol{\theta}_{k^*}, \quad (5)$$

and the ABC-Wass model-posterior by $\pi_{\varepsilon_n}(M_{k^*} | \mathbf{y}) = N_{k^*}(n) / \sum_j N_j(n)$.

We prove that, under Assumptions (A1)–(A4) and for any sequence $\varepsilon_n \rightarrow 0$ with eventually $\varepsilon_n < \min_{k \neq 0} \delta_{k^*} / 2$, one has

$$\pi_{\varepsilon_n}(M_0 | \mathbf{y}) \xrightarrow{P} 1.$$

The proof has two parts: (i) $N_0(n)$ is bounded away from zero in probability; (ii) for every $k^* \neq 0$, $N_{k^*}(n) \xrightarrow{P} 0$. Together these imply posterior concentration on M_0 .

(i) **Lower bound for $N_0(n)$.** Define

$$q_{0,n} := \mathbb{P}(\mathcal{W}_p(\hat{\mu}_0, \hat{\mu}_{k^*}, \boldsymbol{\theta}_{k^*}) \leq \varepsilon_n).$$

By the triangle inequality,

$$\mathcal{W}_p(\hat{\mu}_0, \hat{\mu}_{k^*}, \boldsymbol{\theta}_{k^*}) \leq \mathcal{W}_p(\hat{\mu}_0, P_{M_0, \boldsymbol{\theta}_0}) + \mathcal{W}_p(\hat{\mu}_{k^*}, \boldsymbol{\theta}_{k^*}, P_{M_0, \boldsymbol{\theta}_0}).$$

Hence, for $a \in (0, \varepsilon_n)$,

$$\{\mathcal{W}_p(\hat{\mu}_0, \hat{\mu}_{k^*}, \boldsymbol{\theta}_{k^*}) > \varepsilon_n\} \subseteq \{\mathcal{W}_p(\hat{\mu}_0, P_{M_0, \boldsymbol{\theta}_0}) > a\} \cup \{\mathcal{W}_p(\hat{\mu}_{k^*}, \boldsymbol{\theta}_{k^*}, P_{M_0, \boldsymbol{\theta}_0}) > \varepsilon_n - a\}.$$

It is possible to choose $a = \varepsilon_n / 2$. Then

$$1 - q_{0,n} \leq \mathbb{P}(\mathcal{W}_p(\hat{\mu}_0, P_{M_0, \boldsymbol{\theta}_0}) > \frac{\varepsilon_n}{2}) + \mathbb{P}(\mathcal{W}_p(\hat{\mu}_{k^*}, \boldsymbol{\theta}_{k^*}, P_{M_0, \boldsymbol{\theta}_0}) > \frac{\varepsilon_n}{2}).$$

By Assumption (A4), $\mathcal{W}_p(\hat{\mu}_0, P_{M_0, \theta_0}) \xrightarrow{p} 0$. For the second term $\mathbb{P}(\mathcal{W}_p(\hat{\mu}_{k^*}, \theta_{k^*}, P_{M_0, \theta_0}) > \frac{\varepsilon_n}{2})$, we can use the Markov's inequality

$$\mathbb{P}(\mathcal{W}_p(\hat{\mu}_{k^*}, \theta_{k^*}, P_{M_0, \theta_0}) > \frac{\varepsilon_n}{2}) \leq \frac{2\mathbb{E}[\mathcal{W}_p(\hat{\mu}_{k^*}, \theta_{k^*}, P_{M_0, \theta_0})]}{\varepsilon_n} \leq \frac{2\Delta_n}{\varepsilon_n} \xrightarrow{n \rightarrow \infty} 0,$$

because, under Assumption (A4), $\Delta_n := \sup_{M_{k^*}, \theta_{k^*}} \mathbb{E}[\mathcal{W}_p(\hat{\mu}_{k^*}, \theta_{k^*}, P_{M_{k^*}, \theta_{k^*}}^{(n)})] = o(\varepsilon_n)$. Thus $q_{0,n} \xrightarrow{p} 1$.

Let U be a neighbourhood of θ_0 with prior mass $\pi_{M_0}(U) > 0$. By continuity of $\theta_{k^*} \mapsto P_{M_0, \theta_{k^*}}$ in \mathcal{W}_p , the same argument shows $\mathbb{P}(\mathcal{W}_p(\hat{\mu}_0, \hat{\mu}_{k^*}, \theta_{k^*}) \leq \varepsilon_n) \rightarrow 1$ uniformly for $\theta_{k^*} \in U$. Hence, by dominated convergence,

$$\int_U \pi_{M_0}(\theta_{k^*}) \mathbb{P}(\mathcal{W}_p(\hat{\mu}_0, \hat{\mu}_{k^*}, \theta_{k^*}) \leq \varepsilon_n) d\theta_{k^*} \xrightarrow{p} \pi_{M_0}(U) > 0,$$

and therefore $N_0(n)$ is bounded away from zero in probability, since $\pi(M_0) > 0$ by Assumption (A2).

(ii) Upper bound for $N_{k^*}(n)$ when $k^* \neq 0$. Fix $k^* \neq 0$ and let $\delta_{k^*} > 0$ be as in Assumption (A1), so that $\mathcal{W}_p(P_{M_0, \theta_0}^{(n)}, P_{M_{k^*}, \theta_{k^*}}^{(n)}) \geq \delta_{k^*}$ for all $\theta_{k^*} \in \Theta_{k^*}$. For any θ_{k^*} , by the reverse form of the triangle inequality, we get:

$$\begin{aligned} \mathcal{W}_p(\hat{\mu}_0, \theta_0, \hat{\mu}_{k^*}, \theta_{k^*}) &\geq \mathcal{W}_p(\hat{\mu}_0, \theta_0, P_{M_{k^*}, \theta_{k^*}}^{(n)}) - \mathcal{W}_p(\hat{\mu}_{k^*}, \theta_{k^*}, P_{M_{k^*}, \theta_{k^*}}^{(n)}) \\ &\geq \mathcal{W}_p(P_{M_{k^*}, \theta_{k^*}}^{(n)}, P_{M_0, \theta_0}^{(n)}) - \mathcal{W}_p(\hat{\mu}_0, \theta_0, P_{M_0, \theta_0}^{(n)}) - \mathcal{W}_p(\hat{\mu}_{k^*}, \theta_{k^*}, P_{M_{k^*}, \theta_{k^*}}^{(n)}). \end{aligned}$$

Hence, for Assumption (A1)

$$\mathcal{W}_p(\hat{\mu}_0, \theta_0, \hat{\mu}_{k^*}, \theta_{k^*}) \geq \delta_{k^*} - \mathcal{W}_p(\hat{\mu}_0, \theta_0, P_{M_0, \theta_0}^{(n)}) - \mathcal{W}_p(\hat{\mu}_{k^*}, \theta_{k^*}, P_{M_{k^*}, \theta_{k^*}}^{(n)}).$$

We are interested in the event

$$\mathcal{W}_p(\hat{\mu}_0, \theta_0, \hat{\mu}_{k^*}, \theta_{k^*}) \leq \varepsilon_n,$$

which is equivalent to considering

$$\mathcal{W}_p(\hat{\mu}_0, \theta_0, P_{M_0, \theta_0}^{(n)}) + \mathcal{W}_p(\hat{\mu}_{k^*}, \theta_{k^*}, P_{M_{k^*}, \theta_{k^*}}^{(n)}) \geq \delta_{k^*} - \varepsilon_n.$$

Without loss of generality, select $\varepsilon_n < \delta_{k^*}/2$, then $\delta_{k^*} - \varepsilon_n > \delta_{k^*}/2$, and

$$\left\{ \mathcal{W}_p(\hat{\mu}_0, \theta_0, \hat{\mu}_{k^*}, \theta_{k^*}) \leq \varepsilon_n \right\} \subseteq \left\{ \mathcal{W}_p(\hat{\mu}_0, \theta_0, P_{M_0, \theta_0}^{(n)}) + \mathcal{W}_p(\hat{\mu}_{k^*}, \theta_{k^*}, P_{M_{k^*}, \theta_{k^*}}^{(n)}) \geq \delta_{k^*}/2 \right\}.$$

By the union bound, we obtain

$$\mathbb{P}\left(\mathcal{W}_p(\hat{\mu}_0, \theta_0, \hat{\mu}_{k^*}, \theta_{k^*}) \leq \varepsilon_n\right) \leq \mathbb{P}\left(\mathcal{W}_p(\hat{\mu}_0, \theta_0, P_{M_0, \theta_0}^{(n)}) \geq \frac{\delta_{k^*}}{4}\right) + \mathbb{P}\left(\mathcal{W}_p(\hat{\mu}_{k^*}, \theta_{k^*}, P_{M_{k^*}, \theta_{k^*}}^{(n)}) \geq \frac{\delta_{k^*}}{4}\right).$$

The first term on the right hand side tends to 0 by Assumption (A4), since $\mathcal{W}_p(\hat{\mu}_0, \theta_0, P_{M_0, \theta_0}^{(n)}) \xrightarrow{p} 0$. For the second term, the Markov's inequality and the definition of Δ_n in Assumption (A4) give

$$\mathbb{P}\left(\mathcal{W}_p(\hat{\mu}_{k^*}, \theta_{k^*}, P_{M_{k^*}, \theta_{k^*}}^{(n)}) \geq \frac{\delta_{k^*}}{4}\right) \leq \frac{4}{\delta_{k^*}} \mathbb{E}\left[\mathcal{W}_p(\hat{\mu}_{k^*}, \theta_{k^*}, P_{M_{k^*}, \theta_{k^*}}^{(n)})\right] \leq \frac{4\Delta_n}{\delta_{k^*}} \xrightarrow{n \rightarrow \infty} 0,$$

uniformly over $\theta_{k^*} \in \Theta_{k^*}$. Therefore $N_{k^*}(n) \xrightarrow{p} 0$.

From part (i) there exists $c > 0$ such that $\mathbb{P}(N_0(n) > c) \rightarrow 1$, while from part (ii) $N_{k^*}(n) \xrightarrow{p} 0$ for each $k^* \neq 0$. Thus $\sum_{k \neq 0} N_k(n) \xrightarrow{p} 0$, and consequently

$$\pi_{\varepsilon_n}(M_0 | \mathbf{y}) = \frac{N_0(n)}{N_0(n) + \sum_{k \neq 0} N_k(n)} \xrightarrow{p} 1,$$

as required. □

Appendix C: Proof of Theorem 3.2

Proof. Consider the misspecified setting where the true data distribution $P_{M_0, \theta_0}^{(n)}$ does not belong to any candidate model $M_k \in \mathcal{M}$. Let $(M^\dagger, \theta^\dagger)$ denote the model–parameter pair that minimizes the Wasserstein distance to the true distribution:

$$(M^\dagger, \theta^\dagger) = \arg \min_{M_k \in \mathcal{M}, \theta_k \in \Theta_k} \mathcal{W}_p(P_{M_0, \theta_0}^{(n)}, P_{M_k, \theta_k}^{(n)}).$$

By Assumption (A4), for large n we have

$$\mathcal{W}_p(\hat{\mu}_{0, \theta_0}, P_{M_0, \theta_0}^{(n)}) \leq \eta^{(n)}, \quad \mathcal{W}_p(\hat{\mu}_{k, \theta_k}, P_{M_k, \theta_k}^{(n)}) \leq \eta_k^{(n)},$$

with $\eta^{(n)}, \eta_k^{(n)} \rightarrow 0$ as $n \rightarrow \infty$, and for $k = 1, \dots, K$.

By the triangle inequality, for any (M_k, θ_k) ,

$$\mathcal{W}_p(\hat{\mu}_{0, \theta_0}, \hat{\mu}_{k, \theta_k}) \geq \mathcal{W}_p(P_{M_0, \theta_0}^{(n)}, P_{M_k, \theta_k}^{(n)}) - \eta^{(n)} - \eta_k^{(n)}.$$

Consider first the case of models far from the best approximation. Let $\delta_k := \mathcal{W}_p(P_{M_0, \theta_0}^{(n)}, P_{M_k, \theta_k}^{(n)}) - \mathcal{W}_p(P_{M_0, \theta_0}^{(n)}, P_{M^\dagger, \theta^\dagger}^{(n)}) > 0$. Then for sufficiently large n , setting the ABC threshold $\varepsilon_n < \delta_k/2$ ensures

$$\mathcal{W}_p(\hat{\mu}_{0, \theta_0}, \hat{\mu}_{k, \theta_k}) \geq \delta_k - \eta^{(n)} - \eta_k^{(n)} > \varepsilon_n.$$

Hence, the ABC acceptance probability for such (M_k, θ_k) vanishes:

$$\mathbb{P}\left(\mathcal{W}_p(\hat{\mu}_{0, \theta_0}, \hat{\mu}_{k, \theta_k}) \leq \varepsilon_n\right) \rightarrow 0.$$

Next, consider models near the best approximation. Consider a Wasserstein neighborhood of the optimal pair:

$$\mathcal{N}_\delta := \{(M_k, \theta_k) : \mathcal{W}_p(P_{M_0, \theta_0}^{(n)}, P_{M_k, \theta_k}^{(n)}) \leq \mathcal{W}_p(P_{M_0, \theta_0}^{(n)}, P_{M^\dagger, \theta^\dagger}^{(n)}) + \delta\}.$$

For sufficiently small δ and large n , by the triangle inequality and empirical convergence,

$$\mathcal{W}_p(\hat{\mu}_{0, \theta_0}, \hat{\mu}_{k, \theta_k}) \leq \mathcal{W}_p(P_{M_0, \theta_0}^{(n)}, P_{M_k, \theta_k}^{(n)}) + \eta^{(n)} + \eta_k^{(n)} \leq \mathcal{W}_p(P_{M_0, \theta_0}^{(n)}, P_{M^\dagger, \theta^\dagger}^{(n)}) + \delta + o(1),$$

so that for small $\varepsilon_n > \delta$,

$$\mathbb{P}\left(\mathcal{W}_p(\hat{\mu}_{0, \theta_0}, \hat{\mu}_{k, \theta_k}) \leq \varepsilon_n\right) \rightarrow 1.$$

Combining these two results, the ABC-Wass posterior concentrates on the neighborhood \mathcal{N}_δ :

$$\pi_{\varepsilon_n}(\mathcal{N}_\delta \mid \mathbf{y}) \xrightarrow{P} 1 \quad \text{as } n \rightarrow \infty.$$

This establishes that, under model misspecification, the ABC posterior asymptotically concentrates on the model–parameter pair $(M^\dagger, \theta^\dagger)$ that best approximates the true distribution in Wasserstein distance. \square

Appendix D: Normal Mean Hypothesis Test

This Appendix presents additional results for Section 4.1 of the main paper, focusing on the case of known variance. Figure 4 shows the confusion matrices for each problem, while Figures 5–10 display boxplots of the estimated posterior probabilities of selecting H_0 across repetitions. Full data ABC methods and ABC-Stat exhibit similar behavior, with high classification accuracy and estimated probabilities of selecting H_0 approaching zero as the true mean θ_0 moves further from zero. When θ_0 is small but non-zero, all methods show substantial uncertainty. In comparison, NN struggles across all cases, ABC-QDA consistently selects H_0 with low uncertainty, and ABC-SA performs better than ABC-QDA and the NN but still shows notable variability in estimated model probabilities.

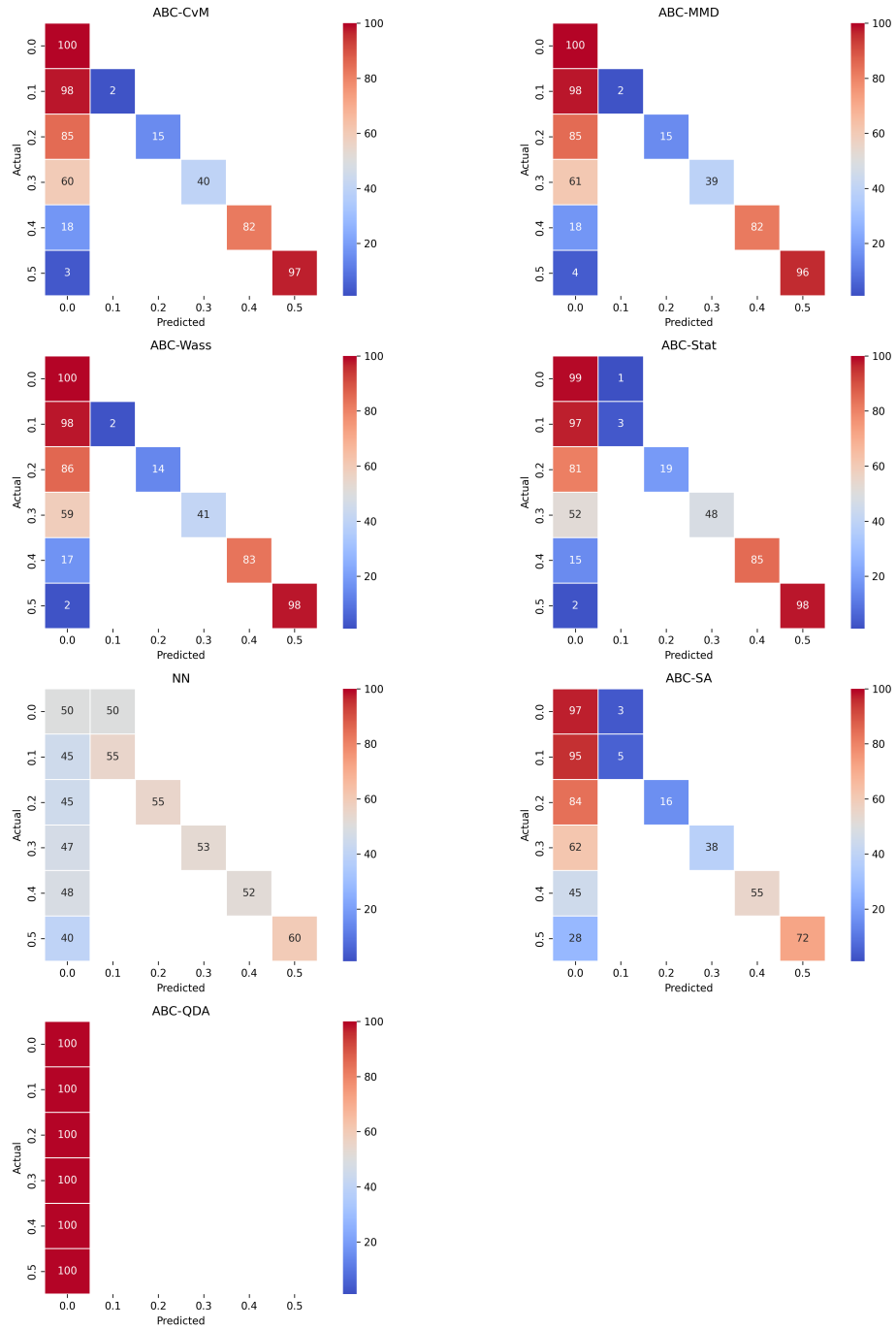


Figure 4: Confusion matrices showing model selection performance for each method in the normal example with $n = 100$. For ABC methods, results are shown using a threshold set at the 1% quantile of simulated distances.

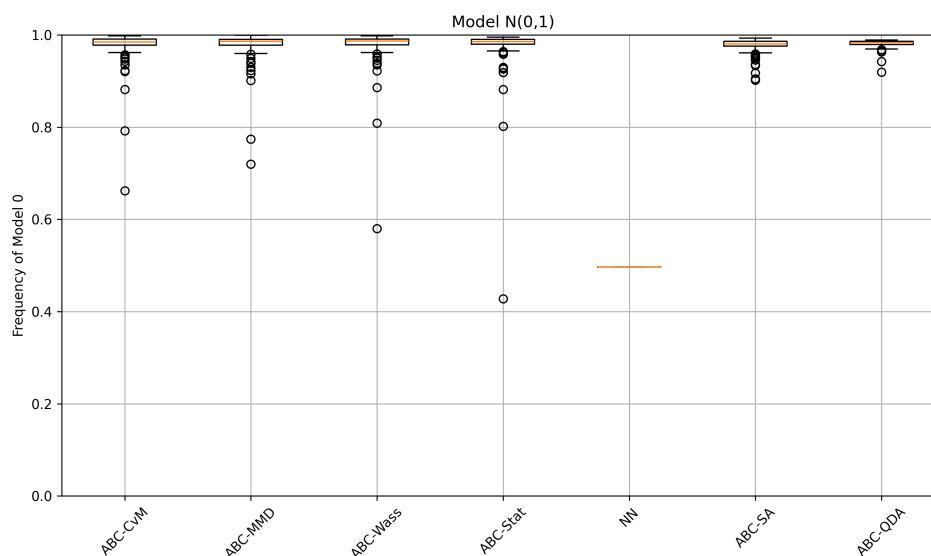


Figure 5: Boxplots of the estimated posterior probability of H_0 across 100 datasets generated from $N(0,1)$, showing the variability of posterior estimates for each method.

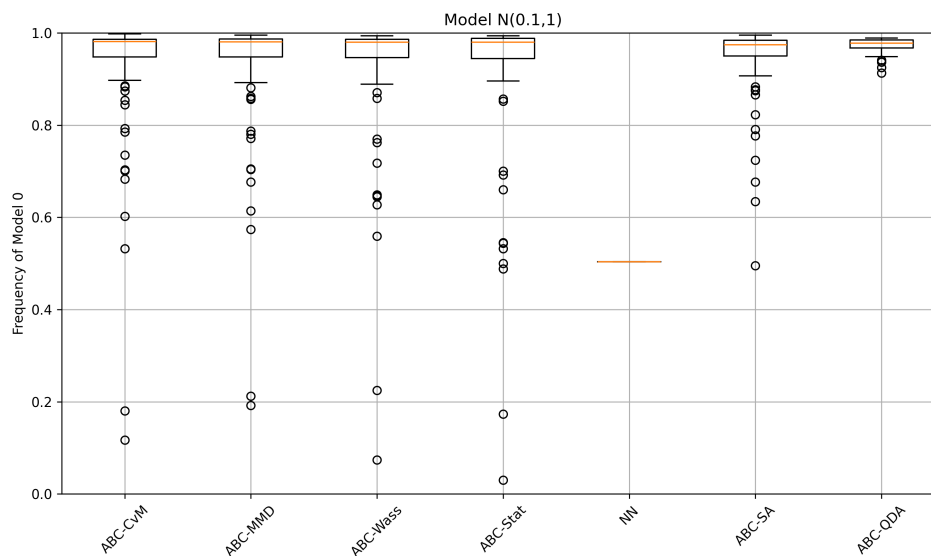


Figure 6: Boxplots of the estimated posterior probability of H_0 across 100 datasets generated from $N(0.1,1)$.

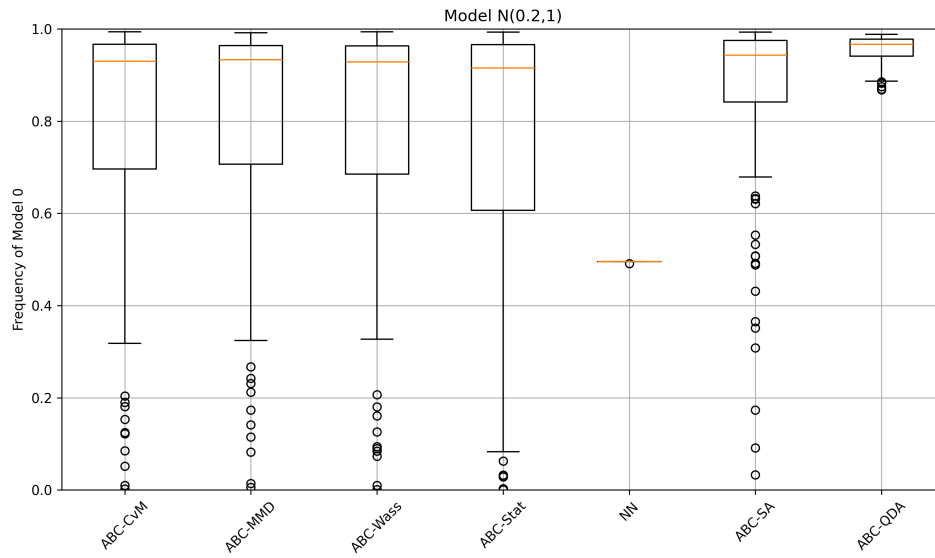


Figure 7: Boxplots of the estimated posterior probability of H_0 across 100 datasets generated from $N(0.2, 1)$.

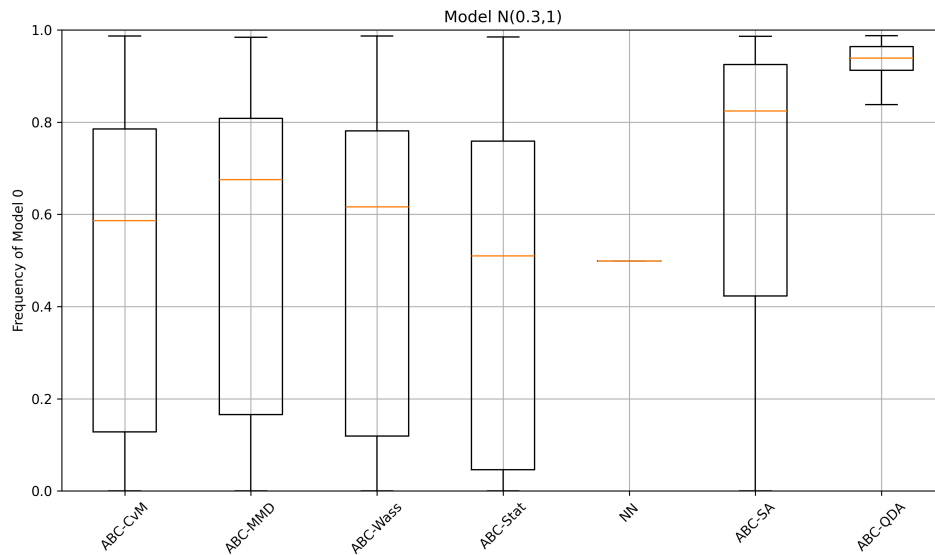


Figure 8: Boxplots of the estimated posterior probability of H_0 across 100 datasets generated from $N(0.3, 1)$.

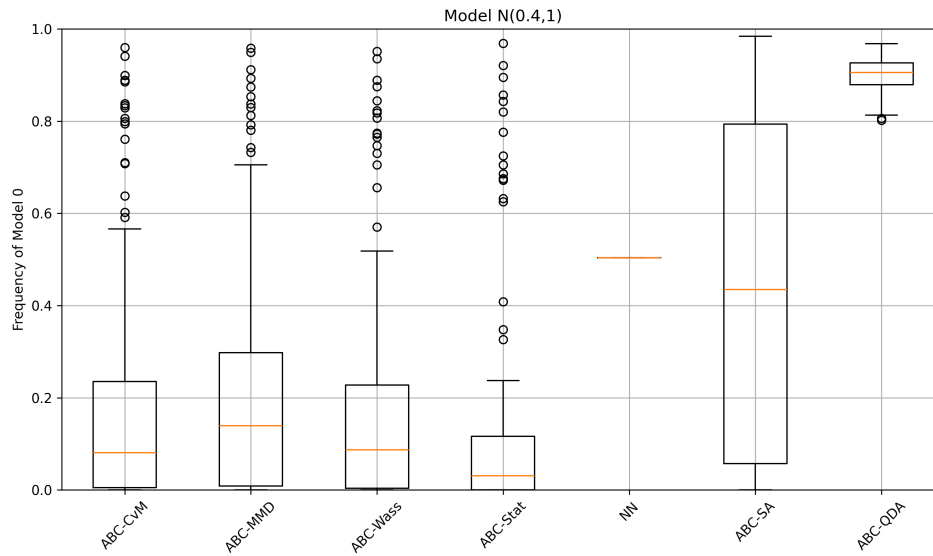


Figure 9: Boxplots of the estimated posterior probability of H_0 across 100 datasets generated from $N(0.4, 1)$.

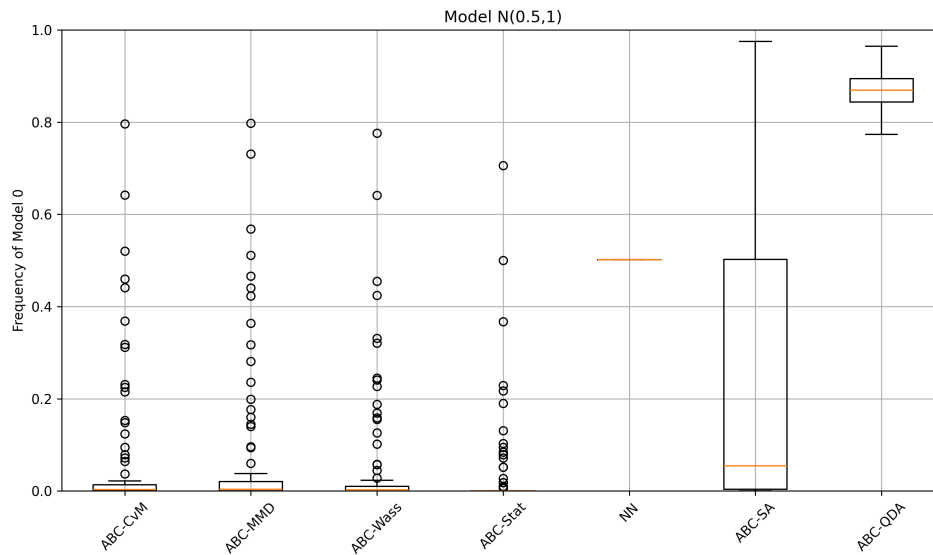


Figure 10: Boxplots of the estimated posterior probability of H_0 across 100 datasets generated from $N(0.5, 1)$.

Appendix E: Exponential Family Model Selection

Figure 11 shows the confusion matrices for the exponential family example, confirming the results reported in the main paper: full data ABC approaches achieve near-perfect classification accuracy, closely matching ABC-Stat. In contrast, ABC-SA and ABC-QDA show lower classification performance, while NN exhibits clear signs of model confusion. The boxplots of the estimated posterior probabilities (Figures 12–14) reveal that all methods display a similar variability. Across methods, the gamma model (M_3) is the easiest to identify (not for NN, which prefers the exponential model to the gamma model even when the data are generated from M_3), with estimated posterior probabilities close to one in most cases. Models M_1 and M_2 are more challenging to recognize, exhibiting higher variability and less consistent model selection.

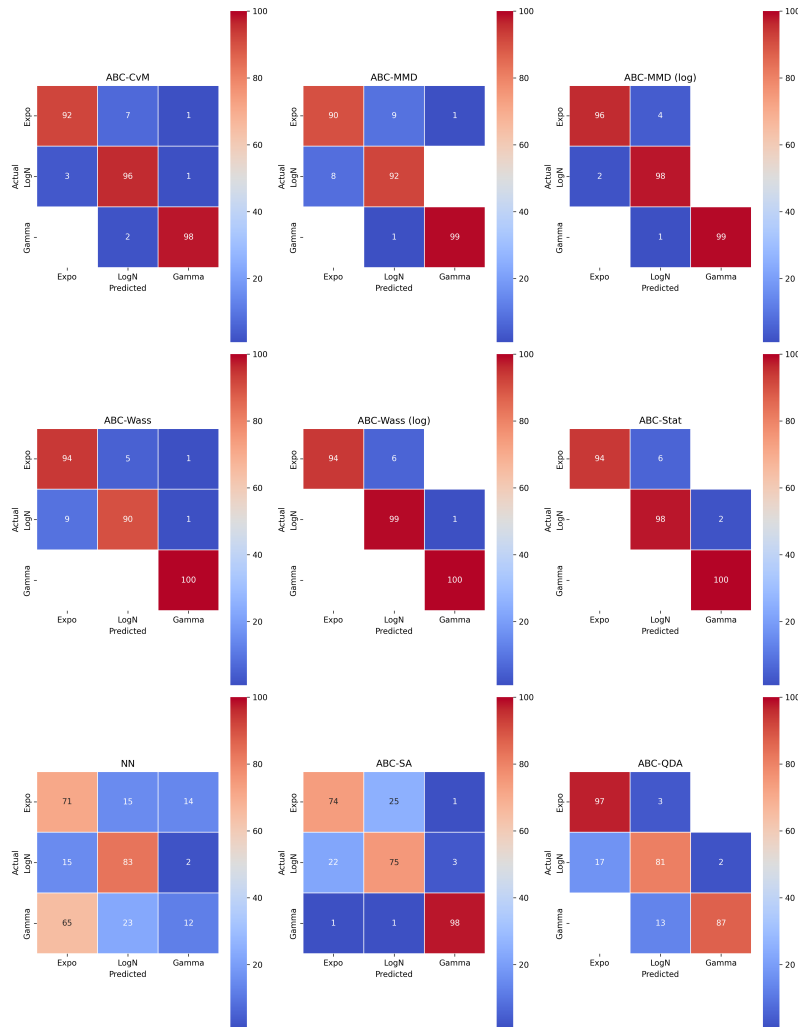


Figure 11: Confusion matrices for model selection in the exponential family example with $n = 100$. ABC methods are shown using a threshold corresponding to the 0.1% quantile of distances.

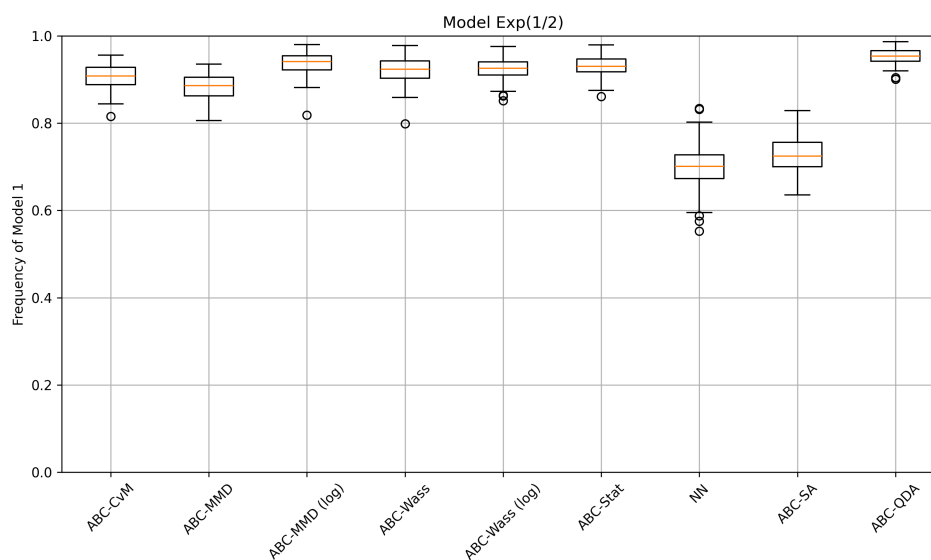


Figure 12: Boxplots of the estimated posterior probability of model M_1 across 100 datasets generated from $\mathcal{E}xp(1/2)$.

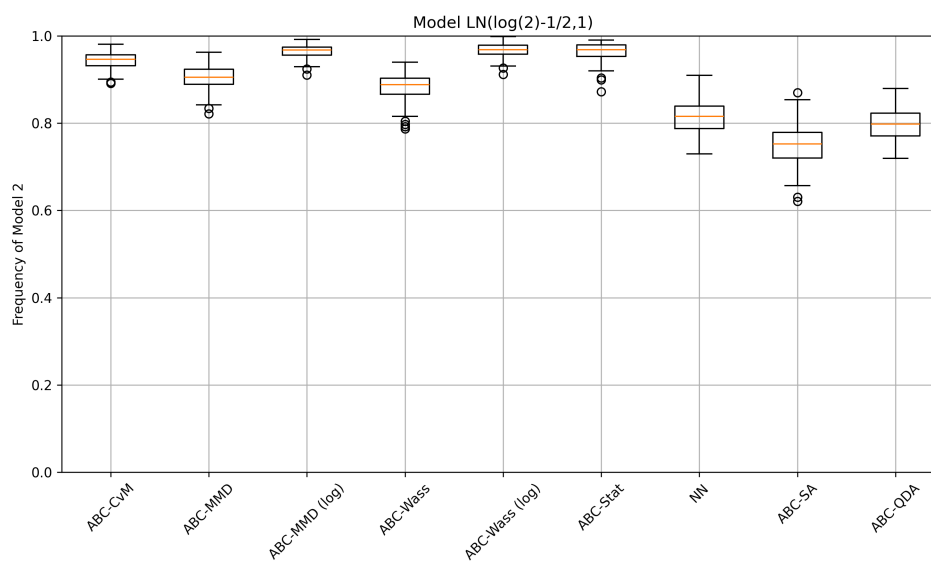


Figure 13: Boxplots of the estimated posterior probability of model M_2 across 100 datasets generated from $\mathcal{LN}(\log(2) - 1/2, 1)$.

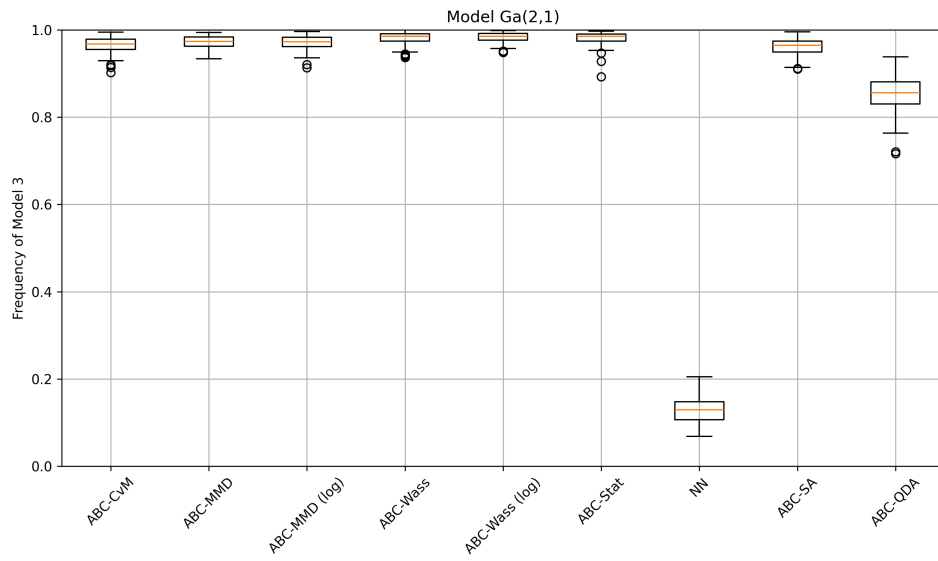


Figure 14: Boxplots of the estimated posterior probability of model M_3 across 100 datasets generated from $\mathcal{G}a(2,1)$.

Appendix F: g -and- k Distribution Model Selection

Figure 15 compares densities computed numerically from model M_1 ($g = 0$) with model M_2 for $g = 1, 2, 3$. The cases $g = 2$ and $g = 3$ are included to highlight how model differences become more pronounced as g increases, whereas for $g = 1$ the densities remain close, suggesting that distinguishing between M_1 and M_2 can be difficult.

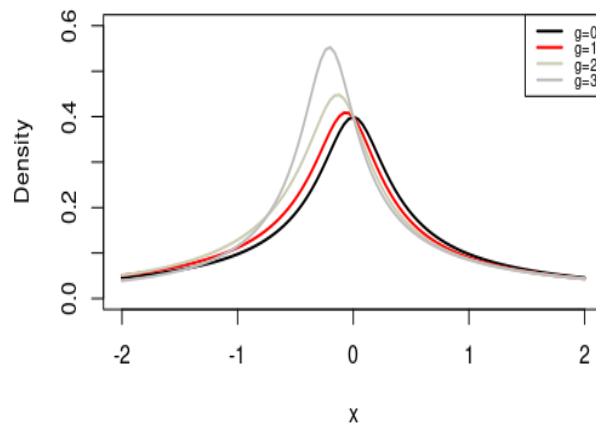


Figure 15: Comparison of g -and- k densities under M_1 ($g_0 = 0$) and M_2 ($g_0 = 1, 2, 3$), with $k = 2$ for all models.

The confusion matrices (Figure 16 and 17) highlight that classification is considerably more challenging for samples of size $n = 100$ than for $n = 1000$. Among the methods, ABC-Wass consistently performs best, achieving perfect classification for data generated under M_2 when $n = 1000$. By contrast, ABC-QDA appears to struggle with identifying the correct model even with large samples, while NN tends to favor M_1 , leading to systematic misclassification. Within the full data ABC approaches, ABC-MMD shows comparatively weaker performance.

The boxplots of estimated posterior probabilities of the correct model (Figures 18-21) reveal distinct behaviors across methods. All full data ABC approaches and ABC-Stat exhibit similar performance, with comparable variability and a clear tendency for the estimated probabilities to approach 1 as the sample size increases. ABC-MMD shows the largest variability, particularly when $n = 1000$. NN produces extreme probabilities, often close to either 0 or 1, regardless of the true model. ABC-SA exhibits diminished performance for $n = 1000$, likely due to the reduced number of summary statistics used as input

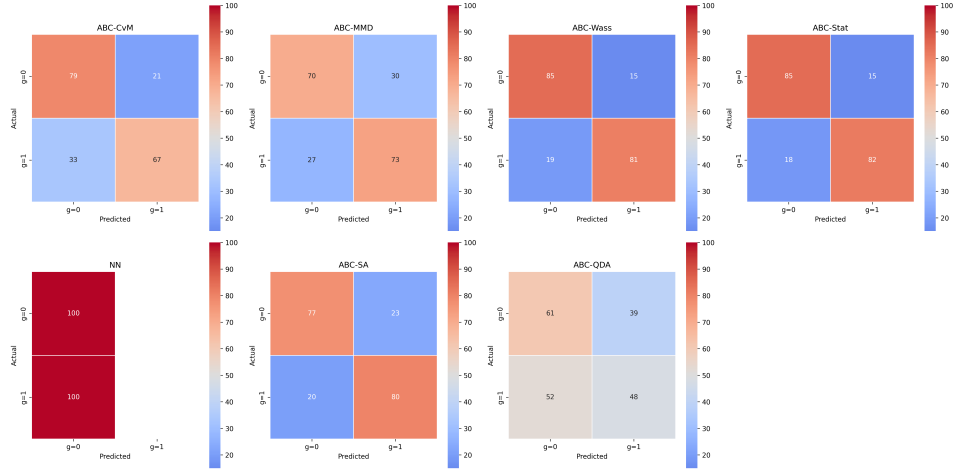


Figure 16: Confusion matrices for model selection in the quantile distribution example with $n = 100$. ABC methods are shown using a threshold corresponding to the 0.1% percentile.

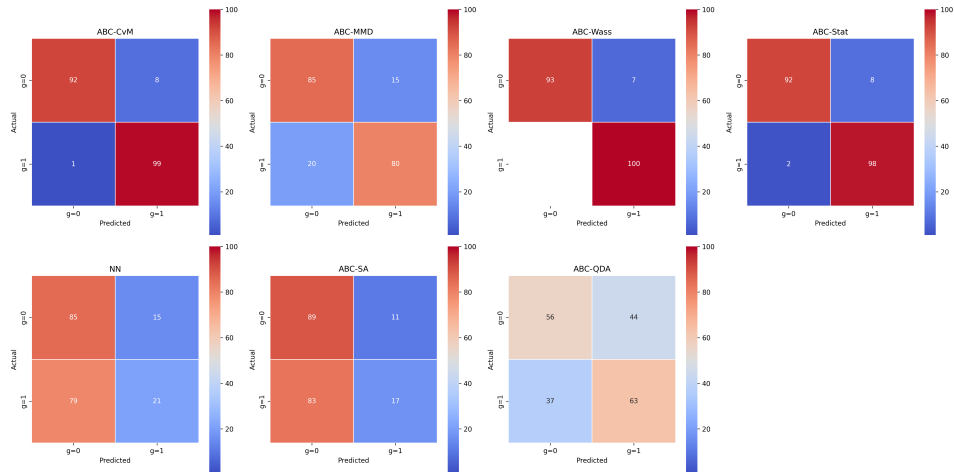


Figure 17: Confusion matrices for model selection in the quantile distribution example with $n = 1000$. ABC methods are shown using a threshold corresponding to the 0.1% percentile.

to limit memory requirements. Finally, ABC-QDA displays the highest variability among all methods, indicating less stable classification.

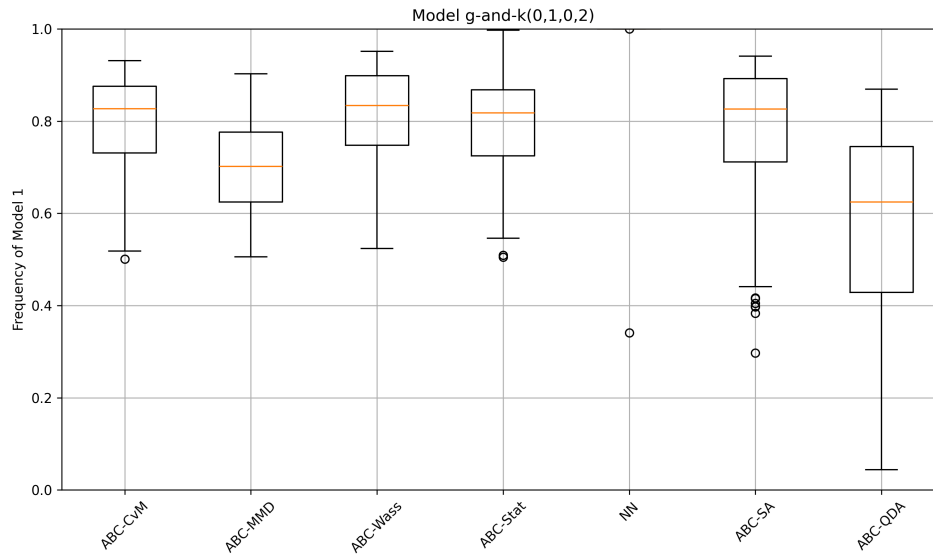


Figure 18: Boxplots of the estimated posterior probability of model M_1 for 100 datasets generated from a $g\text{-and-}k(0,1,0,2)$ distribution with $n = 100$.

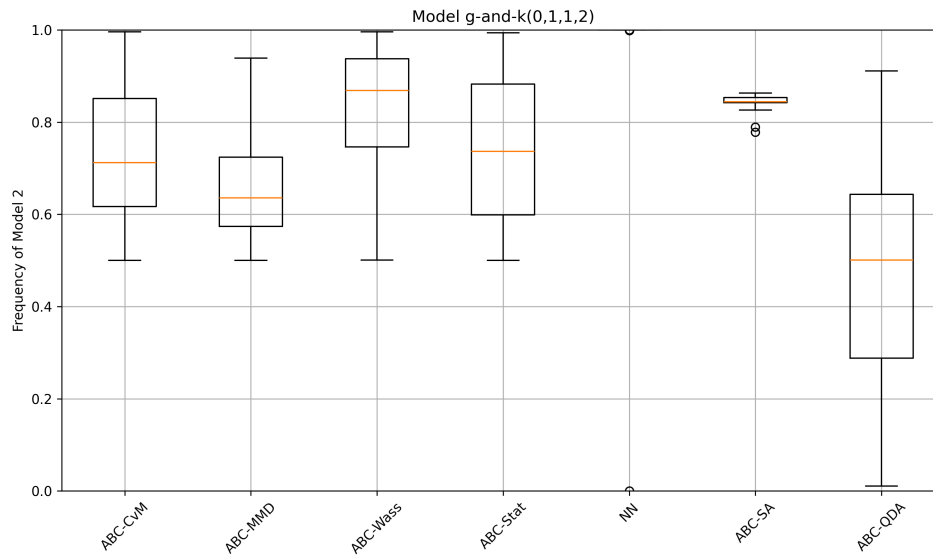


Figure 19: Boxplots of the estimated posterior probability of model M_2 for 100 datasets generated from a $g\text{-and-}k(0,1,1,2)$ distribution with $n = 100$.

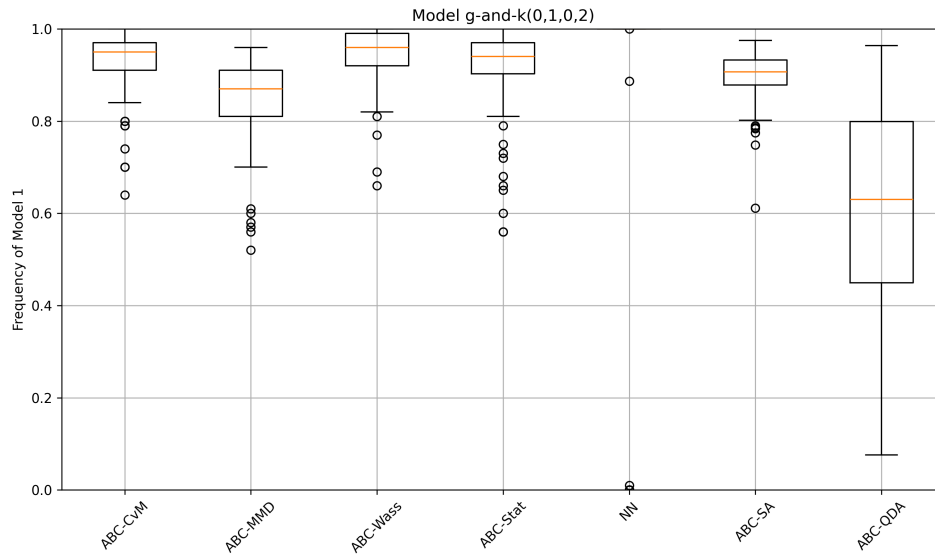


Figure 20: Boxplots of the estimated posterior probability of model M_1 for 100 datasets generated from a $g\text{-and-}k(0,1,0,2)$ distribution with $n = 1000$.

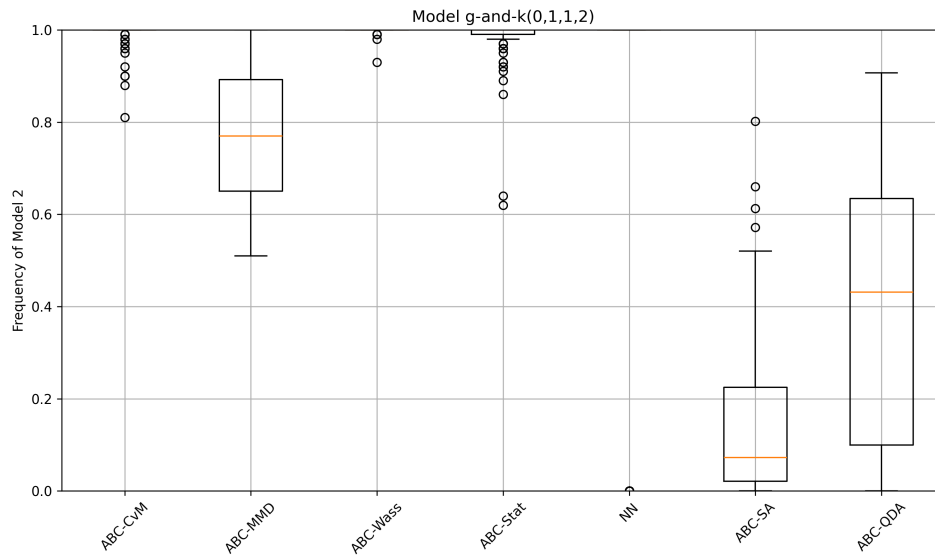


Figure 21: Boxplots of the estimated posterior probability of model M_2 for 100 datasets generated from a $g\text{-and-}k(0,1,1,2)$ distribution with $n = 1000$.

Appendix G: Toad Movement Model Selection

The confusion matrices for the toad movement model example (Figure 22) highlight clear differences in model classification accuracy across methods. ABC-WASS (log) achieves the highest accuracy overall. All full data ABC approaches show nearly perfect classification for model M_2 , with consistently high but slightly lower accuracy for M_1 and M_3 . Misclassifications occur almost exclusively between M_1 and M_3 , reflecting their greater similarity. NN performs poorly, with accuracies close to random guessing. ABC-SA and ABC-Stat achieve performance comparable to the full data ABC approaches, though with a modest reduction in accuracy. In contrast, ABC-QDA performs the worst among the ABC methods.

Similarly, the boxplots of the posterior probabilities of selecting the correct model (Figures 23-25) highlight clear differences between methods. For model M_2 , most approaches yield probabilities close to one, with the exception of the NN method, which produces many outliers at lower values. In contrast, for models M_1 and M_3 , the variability across methods is larger. The NN and ABC-QDA approaches in particular display the widest spread. Among the ABC methods, ABC-WASS (log) consistently achieves the highest medians with minimal variability, while ABC-WASS and ABC-MMD without log transformation show noticeably reduced accuracy for M_1 .

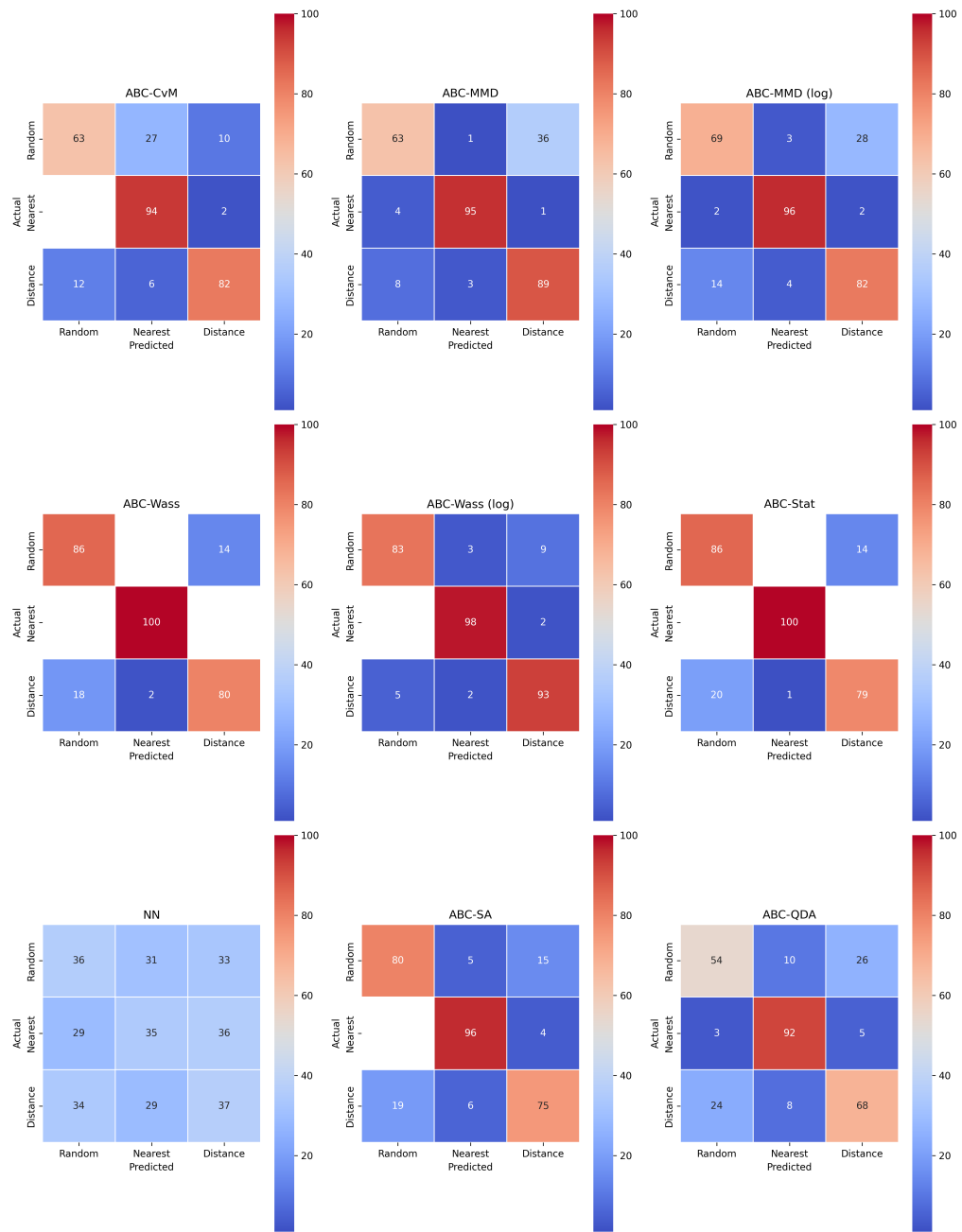


Figure 22: Confusion matrices for model selection across methods for the toad movement example, with ABC approaches using a threshold equal to the 0.1% percentile.

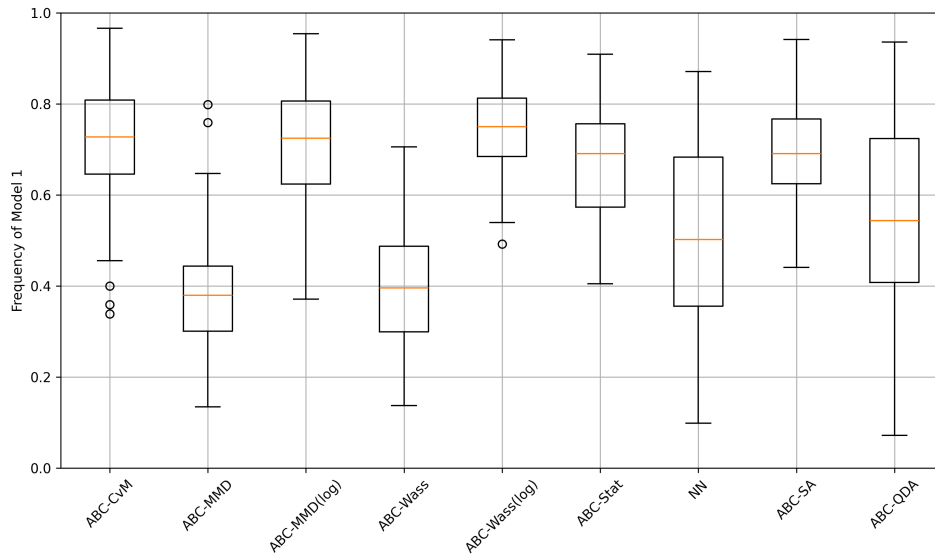


Figure 23: Boxplots of the estimated posterior probabilities of model M_1 across 100 datasets generated from M_1 (random return model).

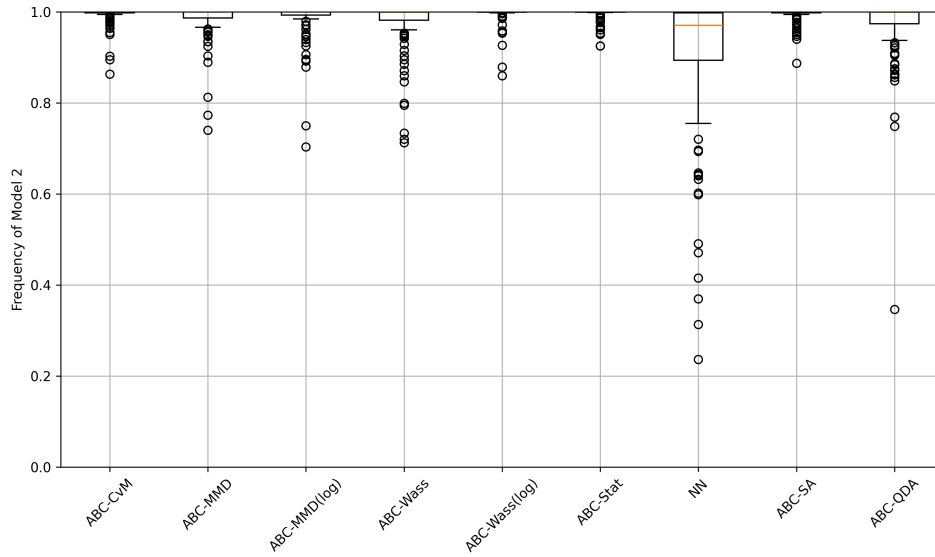


Figure 24: Boxplots of the estimated posterior probabilities of model M_2 across 100 datasets generated from M_2 (nearest return model).

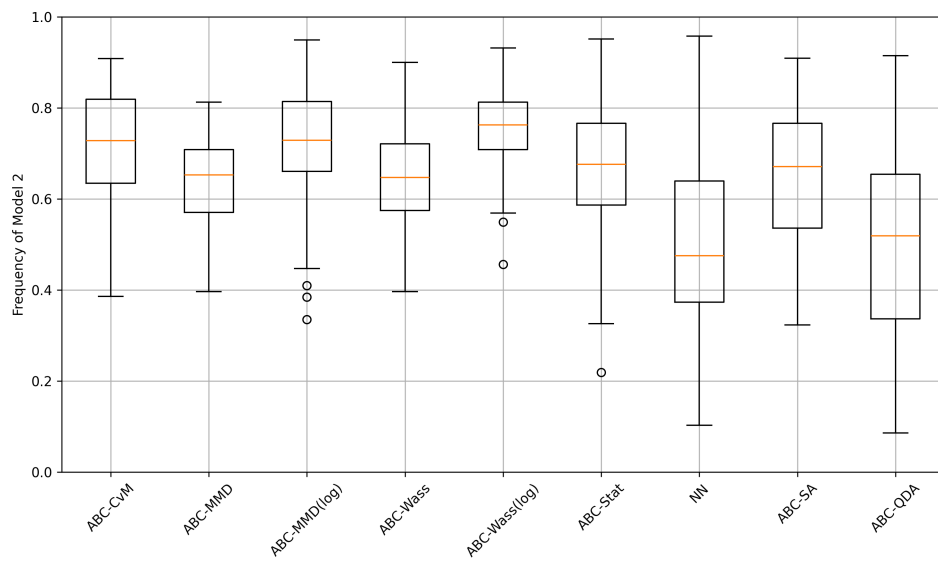


Figure 25: Boxplots of the estimated posterior probabilities of model M_3 across 100 datasets generated from M_3 (distance-based model).

References

- Barber, S., Voss, J., and Webster, M. (2015). “The rate of convergence for approximate Bayesian computation.” *Electronic Journal of Statistics*, 9(1): 80–105. 4
- Bardenet, R., Doucet, A., and Holmes, C. (2017). “On Markov chain Monte Carlo methods for tall data.” *Journal of Machine Learning Research*, (18): 1–43. 4
- Barnes, C., Filippi, S., Stumpf, M., and Thorne, T. (2012). “Considerate approaches to constructing summary statistics for ABC model selection.” *Statistics and Computing*, 22: 1181—1197. 5
- Beaumont, M., Cornuet, J., Marin, J., and Robert, C. (2009). “Adaptive approximate Bayesian computation.” *Biometrika*, 96(4): 983–990. 4
- Beaumont, M. A., Zhang, W., and Balding, D. J. (2002). “Approximate Bayesian Computation in Population Genetics.” *Genetics*, 162(4): 2025–2035. 4
- Bennett, K. L., Shija, F., Linton, Y.-M., Misinzo, G., Kaddumukasa, M., Djouaka, R., Anyaele, O., Harris, A., Irish, S., Hlaing, T., Prakash, A., Lutwama, J., and Walton, C. (2016). “Historical environmental change in Africa drives divergence and admixture of *Aedes aegypti* mosquitoes: a precursor to successful worldwide colonization?” *Molecular Ecology*, 25(17): 4337–4354. 5
- Berk, R. H. (1966). “Limiting behavior of posterior distributions when the model is incorrect.” *The Annals of Mathematical Statistics*, 37(1): 51–58. 14
- Bernton, E., Jacob, P. E., Gerber, M., and Robert, C. P. (2019). “Approximate Bayesian Computation with the Wasserstein Distance.” *Journal of the Royal Statistical Society Series B: Statistical Methodology*, 81(2): 235–269. 2, 7, 8, 25
- Biau, G., C erou, F., and Guyader, A. (2015). “New Insights Into Approximate Bayesian Computation.” *Annales de l’Institut Henri Poincar e*, 51(1): 376–403. 10
- Blum, M. G. and Fran ois, O. (2010). “Non-linear regression models for Approximate Bayesian Computation.” *Statistics and Computing*, 20: 63–73. 2
- Bur es, J. and Larrosa, I. (2023). “Organic reaction mechanism classification using machine learning.” *Nature*, 613(7945): 689–695. 3
- Chambers, J. M., Mallows, C. L., and Stuck, B. W. (1976). “A Method for Simulating Stable Random Variables.” *Journal of the American Statistical Association*, 71(354): 340–344. 18
- Crema, E., Edinborough, K., Kerig, T., and Shennan, S. (2014). “An Approximate Bayesian Computation approach for inferring patterns of cultural evolutionary change.” *Journal of Archaeological Science*, 50: 160–170. 5
- Del Moral, P., Doucet, A., and Jasra, A. (2011). “An adaptive sequential Monte Carlo method for approximate Bayesian computation.” *Statistics and Computing*, 22: 1009 – 1020. 4
- Didelot, X., Everitt, R. G., Johansen, A. M., and Lawson, D. J. (2011). “Likelihood-free estimation of model evidence.” *Bayesian Analysis*, 6(1): 49 – 76. 5, 25
- Donoho, D. L. and Liu, R. C. (1988). “The “Automatic” Robustness of Minimum

- Distance Functionals.” *The Annals of Statistics*, 16(2): 552 – 586. [7](#)
- Drovandi, C. and Frazier, D. (2022). “A Comparison of Likelihood-Free Methods With and Without Summary Statistics.” *Statistics and Computing*, 32(42). [2](#), [4](#), [5](#), [7](#), [13](#), [17](#), [20](#), [24](#)
- Drovandi, C. C., Pettitt, A. N., and Faddy, M. J. (2011). “Approximate Bayesian computation using indirect inference.” *Journal of the Royal Statistical Society Series C: Applied Statistics*, 60(3): 317–337. [4](#)
- Drovandi, C. C., Pettitt, A. N., and Lee, A. (2015). “Bayesian Indirect Inference Using a Parametric Auxiliary Model.” *Statistical Science*, 30(1): 72–95. [4](#)
- Estoup, A., Beaumont, M., Sennedot, F., Moritz, C., and Cornuet, J.-M. (2004). “Genetic Analysis of Complex Demographic Scenarios: Spatially Expanding Population of the Cane Toad *Bufo Marinus*.” *Evolution*, 58(9): 2021–2036. [5](#)
- Fearnhead, P. and Prangle, D. (2012). “Constructing summary statistics for approximate Bayesian computation: semi-automatic approximate Bayesian computation.” *Journal of the Royal Statistical Society Series B: Statistical Methodology*, 74(3): 419–474. [4](#)
- Forbes, F., Nguyen, H. D., Nguyen, T., and Arbel, J. (2022). “Summary statistics and discrepancy measures for approximate Bayesian computation via surrogate posteriors.” *Statistics and Computing*, 32(5): 85. [2](#)
- Fournier, N. and Guillin, A. (2015). “On the rate of convergence in Wasserstein distance of the empirical measure.” *Probability theory and related fields*, 162(3): 707–738. [25](#)
- Frazier, D. T. (2020). “Robust and Efficient Approximate Bayesian Computation: A Minimum Distance Approach.” ArXiv:2006.14126. [2](#), [7](#), [23](#)
- Frazier, D. T., Robert, C. P., and Rousseau, J. (2020). “Model misspecification in approximate Bayesian computation: Consequences and diagnostics.” *Journal of the Royal Statistical Society Series B: Statistical Methodology*, 82(2): 421–444. [3](#)
- Gautestad, A. O. and Mysterud, I. (2005). “Intrinsic Scaling Complexity in Animal Dispersion and Abundance.” *The American Naturalist*, 165(1): 44–55. [18](#)
- Gelman, A. and Shalizi, C. R. (2013). “Philosophy and the practice of Bayesian statistics.” *British Journal of Mathematical and Statistical Psychology*, 66(1): 8–38. [1](#)
- Gleim, A. and Pigorsch, C. (2013). “Approximate Bayesian computation with indirect summary statistics.” University of Bonn Research Paper. [4](#)
- Grelaud, A., Robert, C., Marin, J.-M., Rodolphe, F., and Taly, J.-F. (2009). “ABC likelihood-free methods for model choice in Gibbs random fields.” *Statistics and Computing*, 19(2): 317–336. [5](#)
- Gutmann, M. U., Dutta, R., Kaski, S., and Corander, J. (2018). “Likelihood-free inference via classification.” *Statistics and Computing*, 28: 411–425. [10](#), [15](#)
- Han, C. and Carlin, B. P. (2001). “Markov chain Monte Carlo methods for computing Bayes factors: A comparative review.” *Journal of the American Statistical Association*, 96(455): 1122–1132. [4](#)
- Humphries, N., Queiroz, N., Dyer, J., Pade, N., Musyl, M., Schaefer, K., Fuller, D., Brunnschweiler, J., Doyle, T., Houghton, J., Hays, G., Jones, C., Noble,

- L., Wearmouth, V., Southall, E., and Sims, D. (2010). “Environmental Context Explains Lévy and Brownian Movement Patterns of Marine Predators.” *Nature*, 465: 1066–9. [18](#)
- Jiang, B., Wu, T.-Y., Zheng, C., and Wong, W. H. (2017). “Learning summary statistic for approximate Bayesian computation via deep neural network.” *Statistica Sinica*, 1595–1618. [2](#)
- Joyce, P. and Marjoram, P. (2008). “Approximately Sufficient Statistics and Bayesian Computation.” *Statistical Applications in Genetics and Molecular Biology*, 7(1). [4](#)
- Legramanti, S., Durante, D., and Alquier, P. (2025). “Concentration of discrepancy-based ABC via Rademacher complexity.” [5](#), [6](#), [8](#), [9](#), [23](#), [25](#)
- Marchand, P., Boenke, M., and Green, D. M. (2017). “A stochastic movement model reproduces patterns of site fidelity and long-distance dispersal in a population of Fowler’s toads (*Anaxyrus fowleri*).” *Ecological Modelling*, 360: 63–69. [3](#), [4](#), [18](#), [19](#), [20](#), [22](#), [23](#), [25](#)
- Marin, J.-M., Pillai, N. S., Robert, C. P., and Rousseau, J. (2013). “Relevant Statistics for Bayesian Model Choice.” *Journal of the Royal Statistical Society Series B: Statistical Methodology*, 76(5): 833–859. [5](#), [13](#), [15](#), [16](#)
- Marin, J.-M., Pudlo, P., Estoup, A., and Robert, C. P. (2016). *Likelihood-free Model Choice*, chapter 6. CRC Press Taylor & Francis Group. [12](#)
- Marjoram, P., Molitor, J., Plagnol, V., and Tavaré, S. (2003). “Markov chain Monte Carlo without likelihoods.” *Proceedings of the National Academy of Sciences*, 100(26): 15324–15328. [4](#)
- Martin, G. M., Frazier, D. T., and Robert, C. P. (2024). “Approximating Bayes in the 21st Century.” *Statistical Science*, 39(1): 20–45. [2](#)
- Martin, G. M., McCabe, B. P. M., Frazier, D. T., Maneesoonthorn, W., and Robert, C. P. (2019). “Auxiliary Likelihood-Based Approximate Bayesian Computation in State Space Models.” *Journal of Computational and Graphical Statistics*, 28(3): 508–522. [4](#)
- Miller, N., Estoup, A., Toepfer, S., Bourguet, D., Lapchin, L., derridj, S., Kim, K., Reynaud, P., Furlan, L., and Guillemaud, T. (2005). “Multiple Transatlantic Introductions of the Western Corn Rootworm.” *Science*, 310: 992. [5](#)
- Molnar, C., König, G., Herbinger, J., Freiesleben, T., Dandl, S., Scholbeck, C. A., Casalicchio, G., Grosse-Wentrup, M., and Bischl, B. (2022). *General Pitfalls of Model-Agnostic Interpretation Methods for Machine Learning Models*, 39–68. Springer International Publishing. [1](#)
- Morey, R. D., Rouder, J. N., Pratte, M. S., and Speckman, P. L. (2011). “Using MCMC chain outputs to efficiently estimate Bayes factors.” *Journal of Mathematical Psychology*, 55(5): 368–378. [4](#)
- Nguyen, H. D., Arbel, J., Lü, H., and Forbes, F. (2020). “Approximate Bayesian computation via the energy statistic.” *IEEE Access*, 8: 131683–131698. [2](#), [7](#)
- Nunes, M. A. and Balding, D. J. (2010). “On Optimal Selection of Summary Statistics for Approximate Bayesian Computation.” *Statistical Applications in Genetics and Molecular Biology*, 9(34). [4](#)
- Nunes, M. A. and Prangle, D. (2015). “abctools: an R package for tuning approximate Bayesian computation analyses.” [10](#)

- Park, M., Jitkrittum, W., and Sejdinovic, D. (2016). “K2-ABC: Approximate Bayesian Computation with Kernel Embeddings.” *Proceedings of the 19th International Conference on Artificial Intelligence and Statistics*, PMLR, 51: 398–407. [2](#), [6](#)
- Peters, G. W., Panayi, E., and Septier, F. (2015). *SMC-ABC methods for the estimation of stochastic simulation models of the limit order book*, chapter 15. Chapman and Hall/CRC. [4](#)
- Prangle, D. (2017). “Adapting the ABC distance function.” *Bayesian Analysis*, 12(1): 289–309. [20](#)
- Prangle, D., Fearnhead, P., Cox, M. P., Biggs, P. J., and French, N. P. (2014). “Semi-automatic selection of summary statistics for ABC model choice.” *Statistical Applications in Genetics and Molecular Biology*, 13(1): 67–82. [5](#), [10](#)
- Pritchard, J., Seielstad, M., Perez-Lezaun, A., and Feldman, M. (2000). “Population growth of human Y chromosomes: A study of Y chromosome microsatellites.” *Molecular biology and evolution*, 16: 1791–8. [4](#)
- Raftery, A. E. (1995). “Bayesian Model Selection in Social Research.” *Sociological Methodology*, 25: 111–163. [2](#)
- Ramdas, A., Reddi, S. J., Póczos, B., Singh, A., and Wasserman, L. (2015). “On the decreasing power of kernel and distance based nonparametric hypothesis tests in high dimensions.” In *Proceedings of the AAAI Conference on Artificial Intelligence*, volume 29. [25](#)
- Rayner, G. and MacGillivray, H. (2002). “Numerical maximum likelihood estimation for the g -and- k and generalized g -and- h distributions.” *Statistics and Computing*, 12: 57–75. [15](#)
- Robert, C., Cornuet, J., Marin, J., and Pillai, N. (2011). “Lack of confidence in approximate Bayesian computation model choice.” *Proceedings of the National Academy of Sciences*, 108(37): 15112–15117. [2](#), [5](#), [25](#), [26](#)
- Robert, C. P. (2007). *The Bayesian choice: From decision-theoretic foundations to computational implementation*, volume 2. Springer. [11](#)
- Sheehan, S. and Song, Y. S. (2016). “Deep learning for population genetic inference.” *PLoS Computational Biology*, 12(3): e1004845. [2](#)
- Sims, D. W., Reynolds, A. M., Humphries, N. E., Southall, E. J., Wearmouth, V. J., Metcalfe, B., and Twitchett, R. J. (2014). “Hierarchical random walks in trace fossils and the origin of optimal search behavior.” *Proceedings of the National Academy of Sciences*, 111(30): 11073–11078. [18](#)
- Sisson, S. A., Fan, Y., and Tanaka, M. M. (2007). “Sequential Monte Carlo without likelihoods.” *Proceedings of the National Academy of Sciences*, 104(6): 1760–1765. [4](#)
- Smith, T., Marshall, L., and Sharma, A. (2014). “Predicting hydrologic response through a hierarchical catchment knowledgebase: A Bayes empirical Bayes approach.” *Water Resources Research*, 50(2): 1189–1204. [4](#)
- Toni, T. and Stumpf, M. P. H. (2010). “Simulation-based model selection for dynamical systems in systems and population biology.” *Bioinformatics*, 26(1): 104–110. [25](#)
- Viswanathan, G., Buldyrev, S., Havlin, S., Luz, M., P. Raposo, E., and Stanley, H. (1999). “Optimizing the Success of Random Searches.” *Nature*, 401: 911–4.

18

- Wasserman, L. (2000). "Bayesian Model Selection and Model Averaging." *Journal of Mathematical Psychology*, 44(1): 92–107. [2](#)
- Wilson, D. J., Gabriel, E., Leatherbarrow, A. J., Cheesbrough, J., Gee, S., Bolton, E., Fox, A., Hart, C. A., Diggle, P. J., and Fearnhead, P. (2008). "Rapid Evolution and the Importance of Recombination to the Gastroenteric Pathogen *Campylobacter jejuni*." *Molecular Biology and Evolution*, 26(2): 385–397. [4](#)